LUND UNIVERSITY

Predictive Capabilities of Computer Models for Simulation of Tunnel Fires

Fridolf, Karl; Wahlqvist, Jonathan

2014

[Link to publication](#)

Total number of authors:
2

Predictive Capabilities of Computer Models for Simulation of Tunnel Fires

Karl Fridolf & Jonathan Wahlqvist

Predictive Capabilities of Computer Models for Simulation of Tunnel Fires

Karl Fridolf
Jonathan Wahlqvist

Lund 2014

Predictive Capabilities of Computer Models for Simulation of Tunnel Fires

Karl Fridolf
Jonathan Wahlqvist

Preface

This report, and the work presented in it, represents the project assignment required for a passing grade in the postgraduate course *Fire safety in underground structures*, given at Lund University, LTH, during 2013 and 2014. The course, which was given to postgraduate students at the Department of Fire Safety Engineering at Lund University as well as students at other universities, aimed to increase the students' understanding of:

1. Physical principles related to fire development and smoke spread in underground structures.
2. Human behaviour in underground structure fires.
3. Principles for the development of toxic products and their effects on people exposed to fire smoke.
4. Important aspects of pedestrian dynamics, as well as different egress modelling approaches and their limitations.

As a final project assignment, the students were required to include all of the above in a report in which relevant mathematical models were developed and applied in order to reproduce a tunnel fire, the resulting smoke spread and evacuation of occupants present in the tunnel at the time of the fire.

In this report, the authors' interpretation of that final task is presented. The authors would like to extend a warm thank you to all personnel involved in the course, and especially Haukur Ingason (course coordinator), Håkan Frantzich and Daniel Nilsson for their help along the way.

Nomenclature

A	Cross sectional area of the tunnel [m²]
c_p	Specific heat capacity [kJ/kg K]
D_{mass}	Mass optical density [m²/kg]
FDS	Fire Dynamics Simluator
h	Lumped heat-transfer coefficient for convected and radiated heat losses [kW/m² K]
H_{ec}	Effective chemical heat of combustion [kJ/kg]
H_T	Net heat of complete combustion [kJ/kg]
x	Distance downstream the fire source [m]
$\dot{m}_a$	Mass flow of air [kg/s]
M_i	Molecular weight of chemical specie i [kg/kmol]
M_a	Molecular weight of air [kg/kmol]
M_{O_2}	Molecular weight of oxygen [kg/kmol]
P	Perimeter of the tunnel [m]
Q	Heat release rate [kW]
τ	Time at which the gas, which reaches position x m at time t s, starts to flow from position $x = 0$ m [s]
t	Time [s]
T_{avg}	Cross sectional averaged gas temperature [°C]
T_a	Ambient temperature [°C]
$T_{avg,x=0}$	Cross sectional averaged gas temperature at the fire source [°C]
$TUFT$	TUnnel Fire Tools
u	Air velocity [m/s]
x	Distance downstream the fire source [m]
$X_{i,avg}$	Cross sectional averaged mole fraction of specie i [-]
X_{O_2}	Cross sectional averaged mole fraction of oxygen [-]
χ	Ratio of chemical heat of combustion to net heat of complete combustion [-]
Y_i	Mass yield of specie i [kg/kg]

Table of Contents

1. Introduction

Fires in underground structures, such as underground transportation systems for road and rail vehicles (e.g., tunnels), pose a serious threat to people occupying these facilities. This is not the least demonstrated by past fires (Bergqvist, 2000, 2001; Carvel & Marlair, 2011; Dix, 2010; Donald & Canter, 1990; Duffé & Marec, 1999; Fennell, 1988; Fermaud, Jenne, & Müller, 1995; Larsson, 2004; Rohlén & Wahlström, 1996; Schupfer, 2001; Statens Haverikommission, 2009; Voeltzel, 2002; von Hall G., 2000; Wildt-Persson, 1989). As an example, the fire load is often much higher than for traditional buildings, see for example Ingason and Lönnermark (2012), and the venting possibilities of the fire generated products and smoke are small. In addition, evacuation possibilities are complicated by the fact that the available evacuation routes often are less than in traditional buildings, and furthermore that the fire rescue service will be of little assistance during the evacuation.

Due to the nature of underground facilities, performance-based design solution verification is more or less always required in order to assess life safety and related safety concepts. This verification is likely to include the assessment of a number of fire and evacuation scenarios in order to evaluate the performance of the facility. As computational models often are used, this in turn requires that the existing fire and evacuation models available are validated for the purpose of the type of assessment, i.e., that the models considered has the capability to reproduce true, objective and reliable results related to, for example, temperature, toxicity and visibility. However, in relation to traditional buildings, current models are rarely validated for, e.g., tunnel fires, most likely due to the lack of existing experimental data. Consequently, the extent of uncertainties related to the model results are, in general, unknown.

The purpose of this report is, therefore, to study and to illustrate the model uncertainty in terms fire dynamics in tunnels for two different models: Fire Dynamics Simulator (FDS), and a simpler computer model developed at Lund University, which in this report termed TUFT (abbreviation for TUnnel Fire Tools). By comparing the results of a real full-scale field fire experiment in a tunnel with output from the two models, the aim of the report is to quantify the predictive capability of the models, and also to give practical recommendations on how the input of these models may be modified in order to better represented fire dynamic properties (such as predicting temperatures, toxicity and visibility) in different parts of a tunnel in the different stages of a fire. The aim of the report is, in addition, to compare the differences in output of the two models, one of which represents a relatively complex model (FDS) that requires a lot of resources to use, and one of which represents a fairly simple model based on one dimensional, empirical, bulk models that requires very little resources to use.

2. Method

In order to meet with the purpose and aims of the report, a method was adopted which allowed real experimental data from a full-scale field fire experiment in a tunnel to be compared with data generated using two different models. The process is described below:

1. Find a full-scale field fire experiment that has been well documented in terms of tunnel and fire properties, as well as gas temperature, toxicity and visibility measurements at a number of positions in the tunnel used.
2. Reproduce the experiment using two different models.
3. Compare the results from the experiment and the models.
4. Conduct a comparative analysis of the two models and study differences in output related to temperature, toxicity and visibility for a number of scenarios in order to evaluate the predicting capabilities of TUFT.

2.1. Full-scale experiment

The full-scale field fire experiment used as a reference in this report is an experiment carried out by SP Fire Technology in a tunnel in Norway in year 2003, more specifically the T4-test (Ingason, Lönnermark, & Ying Zhen, 2011). In the test, 600 corrugated paper cartons equipped with 18000 unexpanded polystyrene cups, and 40 wood pallets (L x W x H: 1200 x 1000 x 150 mm) were burnt in an approximately 1600 m long tunnel, reaching a peak heat release rate of approximately 66 MW. The tunnel used in the experiment was the Runehamar tunnel, which has a height and width ratio corresponding to approximately 6 x 8 m. During the test, the fire was located approximately 1040 m into the tunnel, and mobile fans were used to create a longitudinal velocity corresponding to approximately 2.5 m/s during the fire. Measurements of gas temperatures, gas concentrations and extinction coefficients were performed in a wide range of positions both upstream and downstream the fire, more specifically from -93 m upstream the fire to +465 m downstream the fire. The reader is referred to the original publication for more information on the details.

Based on information reproduced from publications and personal communication with Haukur Ingason, the settings of the experiments are summarized in Table 1. This information made up the basis for the input to the model calculations presented later in the report. The heat release rate curve as presented by (Ingason et al., 2011) is also reproduced below.

Table 1. Variable values used as input to FDS and TUFT where applicable.

	Parameter	Quantity
Tunnel	Length	1600 m
	Width	8 m
	Height	6 m
	Wind speed (after ignition)	2.5 m/s
	Ambient temperature	10 °C
Fire	Growth rate[1] (alpha)	0.606 kW/s^2
	Decay rate[1]	0.0727 kW/s^2
	Peak HRR[1]	66 MW
	Peak HRR time[1]	7 min
	Mass optical density[2]	120 m^2/kg
	Heat of combustion[3]	22.2 MJ/kg
	Chi	0.9
	Yield CO_2[4]	2.0 and 2.01
	Yield CO[4]	0.03
	Yield soot[5]	0.02

1 Translated by authors from Figure 1 (excluding pre-burning time)

2 Parameter varied between 30-120 during the fire (lower in the initial stages of the fire), this is used only by TUFT while FDS uses the soot yield

3 Determined by the authors based on items included in fire (see Appendix A: Deriving Input Data to the Computer Models)

4 Determined by the authors based on analysis of experimental results related to gas concentrations of each substance

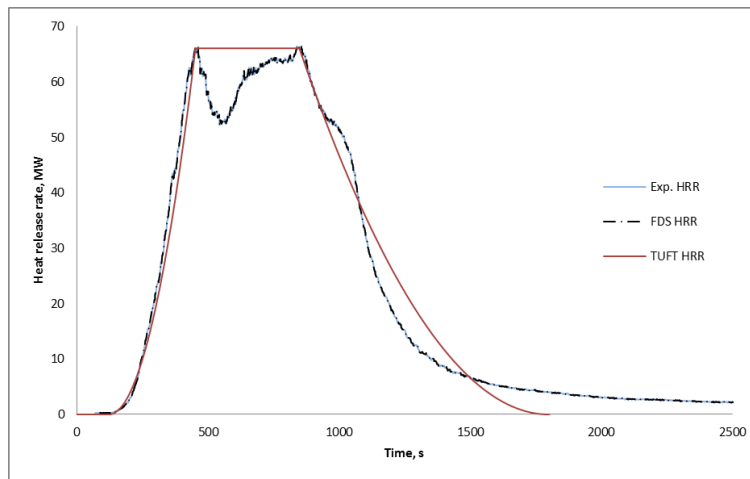5 Only used by FDS instead of mass optical density

Figure 1 Heat release rate as measured in the experiment.

2.2. Comparative scenarios for comparison between FDS and TUFT

In addition to the full-scale experiment scenario, which was reproduced by both models, an additional six scenarios were simulated in both models in order to assess the differences in output related to gas temperature, toxicity and visibility by changes in: a) tunnel width/height proportion; b) tunnel wind speed, and; c) fire growth rate.

In each of the comparative scenarios, only one parameter was varied at a time in a methodology similar to a sensitivity analysis. The reason was to study the isolated effect of the change in parameter, and to reveal the model parameter sensitivity. The comparative scenarios are presented in Table 2. All other parameters (that is not presented in the table) were the same as in the full-scale scenario.

Table 2. Six different scenarios were studied in the comparative analysis. In each scenario, only one parameter was varied at a time. The rest were kept constant with their values as described in

Scenario	Modification
1	Width = 2 m
2	Height = 3 m
3	Wind speed = 0.5 m/s
4	Wind speed = 4 m/s
5	Growth rate = 0.047 kW/s²
6	Growth rate = 0.19 kW/s²

2.3. Measurements

Measurements of various parameters were done upstream as well as downstream the fire in the full-scale field fire experiment (Ingason et al., 2011). In this report, however, only the measurements done downstream the fire is considered. In each simulation, independent of whether it was performed using FDS or TUFT, data on gas temperature, toxicity and visibility was collected at positions determined by the measurement locations of the full-scale field experiment. Measurement positions downstream the fire (in relation to the fire source), are described in Table 3.

Table 3. Measurement positions downstream the fire in the experiment and the simulations respectively.

Position (down-stream fire) [m]	Full-scale experiment	Simulations
27	Gas temperature	Gas temperature, gas concentrations and extinction coefficient
47	Gas temperature	Gas temperature, gas concentrations and extinction coefficient
77	Gas temperature	Gas temperature, gas concentrations and extinction coefficient
107	Gas temperature	Gas temperature, gas concentrations and extinction coefficient
157	Gas temperature	Gas temperature, gas concentrations and extinction coefficient
207	-	Gas temperature, gas concentrations and extinction coefficient
257	Gas temperature	Gas temperature, gas concentrations and extinction coefficient
307	-	Gas temperature, gas concentrations and extinction coefficient
357	Gas temperature	Gas temperature, gas concentrations and extinction coefficient
407	-	Gas temperature, gas concentrations and extinction coefficient
465	Gas temperature, gas concentrations and extinction coefficient	Gas temperature, gas concentrations and extinction coefficient

For comparative reasons, the positions 207 m, 307 m, and 407 m were included in all simulations. In contrast to the full-scale field experiment, predictions were made related to gas temperature, gas concentrations and extinction coefficient at all positions.

2.4. FDS

Fire Dynamics Simulator (FDS) is a computational fluid dynamics (CFD) model of fire-driven fluid flow. The software solves numerically a large eddy simulation form of the Navier-Stokes equations appropriate for low-speed, thermally-driven flow, with an emphasis on smoke and heat transport from fires. FDS is free software developed by the National Institute of Standards and Technology (NIST) of the United States Department of Commerce, in cooperation with VTT Technical Research Centre of Finland. Smokeview is the companion visualization program that can be used to display the output of FDS.

The first version of FDS was publicly released in February 2000. To date, about half of the applications of the model have been for design of smoke handling systems and sprinkler/detector activation studies. The other half consists of residential and industrial fire reconstructions. Throughout its development, FDS has been aimed at solving practical fire problems in fire protection engineering, while at the same time providing a tool to study fundamental fire dynamics and combustion.

2.4.1. Hydrodynamic Model
FDS solves numerically a form of the Navier-Stokes equations appropriate for low-speed, thermally-driven flow with an emphasis on smoke and heat transport from fires. The core algorithm is an explicit predictor-corrector scheme, second order accurate in space and time. Turbulence is treated by means of Large Eddy Simulation (LES). It is possible to perform a Direct Numerical Simulation (DNS) if the underlying numerical mesh is fine enough. LES is the default mode of operation.

2.4.2. Combustion Model
For most applications, FDS uses a single step, mixing-controlled chemical reaction which uses three lumped species (a species representing a group of species). These lumped species are air, fuel, and products. By default the last two lumped species are explicitly computed. Options are available to include multiple reactions and reactions that are not necessarily mixing-controlled.

2.4.3. Radiation Transport
Radiative heat transfer is included in the model via the solution of the radiation transport equation for a grey gas, and in some limited cases using a wide band model. The equation is solved using a technique similar to finite volume methods for convective transport, thus the name given to it is the Finite Volume Method (FVM). Using approximately 100 discrete angles, the finite volume solver requires about 20 % of the total CPU time of a calculation, a modest cost given the complexity of radiation heat transfer. The absorption coefficients of the gas-soot mixtures are computed using the RadCal narrow-band model. Liquid droplets can absorb and scatter thermal radiation. This is important in cases involving mist sprinklers, but also plays a role in all sprinkler cases. The absorption and scattering coefficients are based on Mie theory.

2.4.4. Geometry
FDS approximates the governing equations on a rectilinear mesh. Rectangular obstructions are forced to conform to the underlying mesh.

2.4.5. Multiple Meshes
This is a term used to describe the use of more than one rectangular mesh in a calculation. It is possible to prescribe more than one rectangular mesh to handle cases where the computational domain is not easily embedded within a single mesh. It is possible to run an FDS calculation on more than one computer using the Message Passing Interface (MPI).

2.4.6. Boundary Conditions
All solid surfaces are assigned thermal boundary conditions, plus information about the burning behavior of the material. Heat and mass transfer to and from solid surfaces is usually handled with empirical correlations, although it is possible to compute directly the heat and mass transfer when performing a Direct Numerical Simulation (DNS).

2.5. TUFT
The second model include in the report is simple computer model, a tunnel fire tool, developed at Lund University (Fridolf & Frantzich, 2014). The model is developed in object-oriented Java, and does in essence include four basic sub models: 1) a tunnel geometry model; 2) a fire model; 3) an evacuation model; and 4) a fire rescue operations model.

The tunnel sub model is simply a physical description of the tunnel of consideration: the tunnel length, width, and height, wind speed and ambient temperature. As the name suggest, the fire sub model is a description of the design fire of the scenario being evaluated. In essence, the following parameters are defined before a simulation: the position of the fire; the growth rate and maximum heat release rate; the heat of combustion; the smoke potential, and; the yields of CO_2, CO and HCN. When the scenario has

been defined, the model is able to calculate various parameters related to fire dynamics in tunnels, such as backlayering distance upstream the fire and gas temperature, heat flux, visibility (extinction coefficient) and mole fractions of different species at any position in the tunnel. The underlying equations used in the model are in essence based on the research performed by Ingason, which is summarized in (Ingason, 2012). These are rather coarse, one-dimensional bulk equations, which per definition are not as exact as CFD models. In this report, some of these equations are used to a greater extent than others, and are therefore shortly presented below.

2.5.1. Gas temperature

In TUFT, the cross sectional averaged gas temperature is calculated based on the governing energy equation for one-dimensional bulk flow in a tunnel. By assuming a lumped heat-transfer coefficient for both convective and radiative heat losses, and by assuming that the wall temperature always is the same as the ambient temperature in the tunnel, the following equation is used to derive the gas temperature [°C] at a position x m downstream the fire t s into the fire development:

$$T_{avg}(x,t) = T_a + [T_{avg,x=0}(\tau) - T_a]e^{-(hPx/\dot{m}_a c_p)}$$
Equation 1

This equation requires that the average gas temperature at the fire source (i.e., x = 0 m) has been evaluated in a preceding calculation at a time corresponding to the time it will take to transport the heat generated at the fire location to the distance x m. This is a two-step calculation in which first of all the transportation time of the gases is determined, where after the cross sectional averaged gas temperature at the fire source is calculated with the equations:

$$\tau = t - (x/u)$$
Equation 2

$$T_{avg,x=0}(\tau) = T_a + \frac{2}{3}\frac{Q(\tau)}{\dot{m}_a c_p}$$
Equation 3

As can be seen, it is assumed that one third of the total heat release rate of the fire is lost due to radiation. Furthermore, it is assumed that the time it will take to transport the heat generated at the fire to the location x m is dependent on the ventilation conditions (i.e., x/u). No effects of increased velocity due to increased gas temperature, which may be particularly important in regions close to the fire, has been considered.

2.5.2. Gas concentration

Estimation of the cross sectional averaged mole fraction of different species is done based on the following general equation:

$$X_{i,avg} = Y_i \frac{M_i}{M_a} \frac{Q(\tau)}{\dot{m}_a \chi H_T}$$
Equation 4

Similarly, the cross sectional averaged mole fraction of oxygen is calculated using the equation:

$$X_{O_2} = 0.2095 - \frac{M_a}{M_{O_2}} \frac{Q(\tau)}{\dot{m}_a 13100}$$
Equation 5

In TUFT, only one fixed yield is used for the entire fire scenario. In other words, it is up to the user to define the type of fire.

2.5.3. Visibility (extinction coefficient)

Calculation of the cross sectional averaged visibility is done in TUFT with the following equation:

$$V = 0.87 \frac{uAH_{ec}}{Q(\tau)D_{mass}}$$
Equation 6

The calculated value corresponds to the visibility for objects such as walls, floors and doors or reflecting signs (as opposed to light-emitting signs, for which the visibility distance would be approximately twice as high).

2.5.4. Evacuation

In this report, few parts of the evacuation model of TUFT are used. Consequently, only a brief summary of the sub model is included here. Interested readers are referred to other publications for more information about the sub model, as well as the rescue operation model (by, for example, Fridolf and Frantzich (2014)).

When TUFT is used to perform an evacuation simulation, the effects of the fire at a specific position x m (where x represents the position of the evacuee) is determined for each time step (1 s) of the simulation. In this case, x represents the position of the evacuee in that time step, and the above equations are (among others) used to evaluate the fire effects on the evacuee. Note that x changes as the evacuee moves during the evacuation.

In a first step, TUFT determines whether or not the evacuee is downstream or upstream the fire. If the evacuee is at a position upstream the fire, the model only models transportation and does not take into account fire effects (the exception is when the evacuee is < 50 m from the fire source, for which the radiating effects of the fire is evaluated using the FED methodology). If, however, the evacuee is at a position downstream the fire, the model starts by evaluating the visibility conditions. Depending on the visibility, the distance moved for the time step of 1 s is determined according to (Fridolf, Andrée, Nilsson, & Frantzich, 2013). FED calculations of asphyxiants as well as heat (including heat transfer from the gases, and radiation from the fire source if the evacuee is < 50 m from the fire) is then performed and added to the evacuee's total dose (accumulated from previous time steps). In the end of each time step, the model controls whether or not the evacuee is incapacitated, dead or evacuated to safety. An evacuee is determined evacuated when the agent has reached either an emergency exit (if available in the scenario) or any of the tunnel portals.

If more than one evacuee is considered in the simulation, it should be noted that each agent acts isolated and no communication, group effects, etc. is considered. Furthermore, the evacuee is considered to have reached safety when x corresponds to the position of the safe location (either the closest emergency exit or any of the tunnel portals). Thus, no flow effects, e.g., for modelling the flow of people through doors, is considered in the model.

3. Results

In this section, the findings of the study are presented in two parts. The first part includes the experimental results of the full-scale field study, including the simulation results of FDS and TUFT based on the in data presented in Table 1. The second part includes the results of the comparative study between FDS and TUFT for the six different scenarios described in Table 2.

3.1. Part 1: Comparison between full-scale field experiment and the models

In this section, the results related to the full-scale field study and the simulation results of FDS and TUFT. Firstly, some comments on the use of FDS are presented. Secondly, the results related to gas temperature, gas concentrations and extinction coefficient is presented in figures including both the experimental findings and the simulation results. Finally, a summary of the most important findings is presented.

3.1.1. Comments on the use of FDS

In this initial comparison a very coarse grid has been used in FDS throughout in order to reduce the computational time. This will most likely lead to under-estimated temperatures near and in the flame region and probably initially under estimated mixing of gases and the hot and cold layer.

As described in *Appendix A: Deriving Input Data to the Computer Models,* FDS used a mixture of wood (the pallets and the cardboard) and polystyrene (the cups) to represent the chemical composition of the fuel source. Since wood and paper can differ quite a lot in its chemical composition this could be a large source of error and could have a significant effect on the oxygen consumption and CO_2 concentration. It was also not known at which time each material actually combusted which increases the uncertainty.

A lot of simplifications regarding the geometry were made to be able to fit the Cartesian grid used by FDS, e.g. the tunnel was estimated to be rectangular and the protective insulation setup was simplified to avoid numerical instability.

The simplified, one-step infinitely fast combustion model in FDS was used and hence the CO-production was simply a product of the specified CO-yield and the mass loss rate from the fire source, as in no predictive capabilities regarding under-ventilated fires etc. was used.

3.1.2. Gas temperature

As described above in Table 3, measurements of the gas temperature were done at various positions in the tunnel in the full-scale field experiment. These measurements are termed according to the analogy "Exp. | T, +xm" in Figure 2 – Figure 10 below, where x marks the position downstream the fire. The vertical position of the measurement device in the experiment is in some occasions unknown, in other known. Where known, the vertical position is explicitly stated according to the analogy "Exp. | T ym, xm" where y marks the vertical position (measured from the floor [authors interpretation]). The output from FDS is similarly termed "FDS | T avg/max, +xm" where avg corresponds to the cross-sectional averaged temperature (based on all measurement devices at the position) and max corresponds to the maximum temperature in the cross section, x m downstream the fire. The output from TUFT is termed according to "TUFT | T, +xm" and always represents a cross-sectional averaged value x m downstream the fire source.

Studying the figures below, it can be concluded that both FDS and TUFT underestimate the gas temperature in the closer regions of the fire. At the position 27 m downstream the fire, the average temperatures are in the region 50-100 °C lower than in the experiment. It is, however, a bit unclear where the experiment measurement device was located. If this is a value recorded, e.g., close to the ceiling, this could explain the deviation from the simulation results. The difference is, however, even greater at the position 47 m downstream the fire. It is speculated that this is due to incomplete combustion at the source of the fire in the experiment (due to lack of oxygen), which causes unburnt gases to react with oxygen a bit downstream in the tunnel. It is possible that this, in turn, causes flame spread at ceiling height in reality. In any way, TUFT lacks the possibility to take this into account, and FDS can have trouble predict this complex phenomena accurately, especially with the coarse grid size that was used.

A better prediction of the gas temperature is achieved with FDS when the temperature is measured further downstream the fire. At distances 107-157 m downstream the fire, the average output of FDS is a very good prediction of the experiment data. TUFT, on the other hand, tends to more and more underestimate the gas temperature further downstream the fire. It is most likely that this is caused by how the model handles heat transfer to the tunnel walls, see the sub-section *Gas temperature* in the *TUFT* section. In order to get a better prediction of the gas temperature, one way could be to decrease the lumped heat-transfer coefficient in Equation 1 from, e.g., 0.03 to 0.02 W/m² K. The effects of this are discussed in *TUFT and the Effect of the Lumped Heat Transfer Coefficient.*
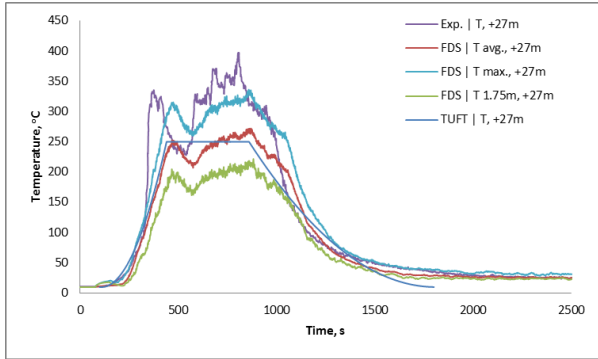
Figure 2. The gas temperature measured 27 m downstream the fire source.
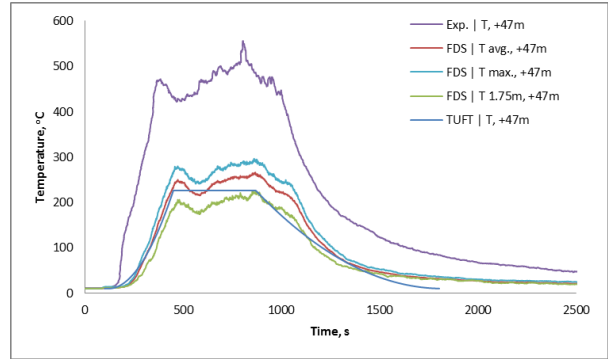
Figure 3. The gas temperature measured 47 m downstream the fire source.
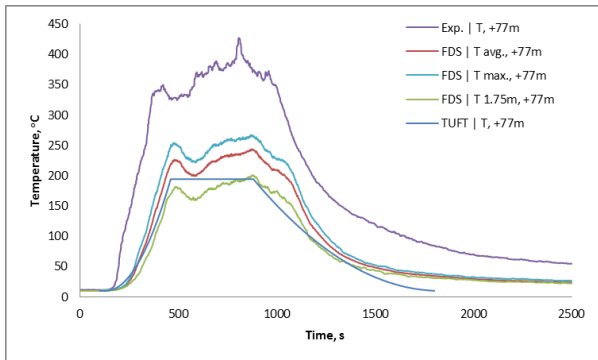
Figure 4. The gas temperature measured 77 m downstream the fire source.
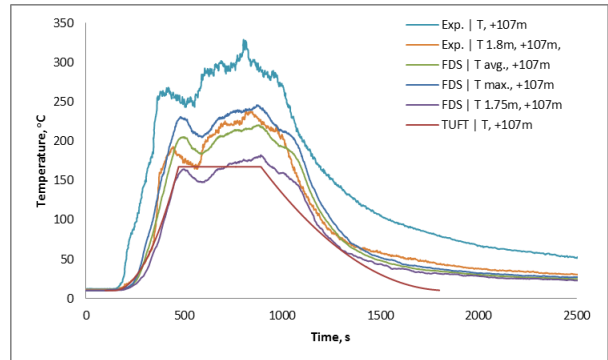
Figure 5. The gas temperature measured 107 m downstream the fire source.
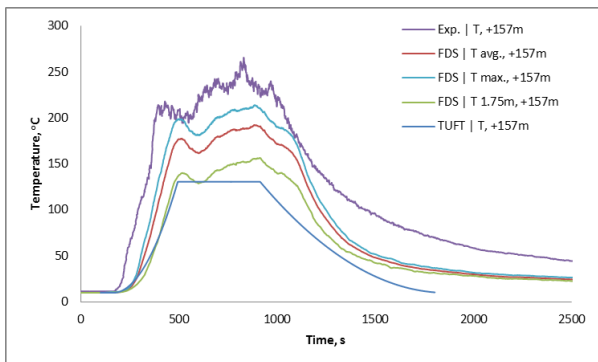
Figure 6. The gas temperature measured 157 m downstream the fire source.
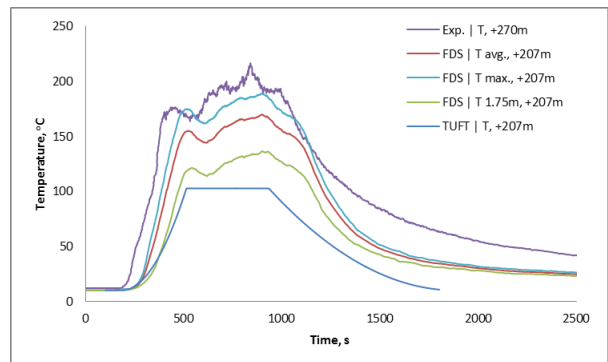
Figure 7. The gas temperature measured 207 m downstream the fire source.
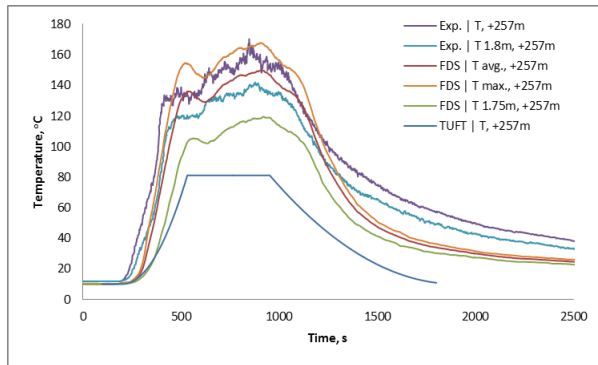
Figure 8. The gas temperature measured 257 m downstream the fire source.
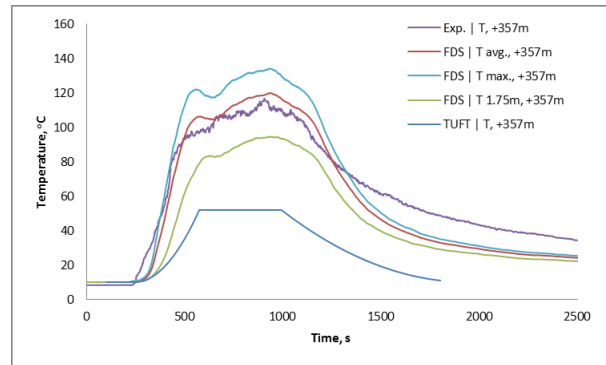
Figure 9. The gas temperature measured 357 m downstream the fire source.
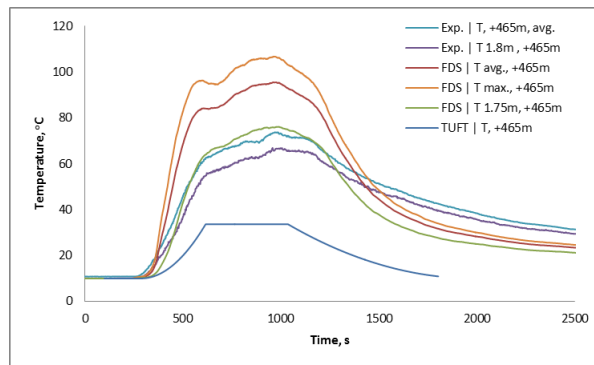
Figure 10. The gas temperature measured 465 m downstream the fire source.

3.1.3. Gas concentrations

In the Runehamar experiment, measurements of the gas concentrations of O_2, CO and CO_2 respectively, were only made at one position in the tunnel (465 m downstream the fire). Therefore, the measurements in FDS and TUFT are only presented for this location below. The measurements are termed according to an analogy similar to what is described above for the measurements of the gas temperature.

As can be seen in Figure 11, both FDS and TUFT overestimates the average gas concentration of O_2 465 m from the fire with about 1 volume percentage. On the other hand, the value conforms to the gas concentration measured at the vertical height corresponding to 1.8 m from the floor, which in (for example) an evacuation simulation would be of most interest as it is at this position evacuating peoples head position might be.

Studying Figure 12, both FDS and TUFT seems to perform very well in terms of predicting the CO_2 volume fraction 465 m downstream the fire. Not only is the maximum value well represented, but also the development of the volume fraction during the first ~500 s. The rather good reproduction of CO_2 concentration is likely explained by the fact that the yield used in the calculation was determined by studying the experimental output from Runehamar.

In terms of prediction of the gas concentration of CO, Figure 13 reveals that both FDS and TUFT are quiet good at predicting the initial increase of CO volume fraction. However, something happens around ~500 s, where the experimental measurements show a rapid decrease of CO gas concentration, which is not captured by FDS or TUFT. The physical explanation could be related to the second stage reaction, where initially produced CO reacts with oxygen as temperatures get higher later into the fire; a phenomena that neither FDS (using the simplified combustion model) nor TUFT has the possibility to capture. Another explanation could be that the fire in the experiment caused an early burn-off of the majority of the plastic materials involved in the scenario (causing a lot of CO to be produced due to the incomplete combustion), and that the later stages of the fire only involved a better combustion of the wooden pallets. In FDS and TUFT, this is not captured, as the material proportions are kept fixed for the

entire fire. Finally, a third possible explanation due to the large difference between the models and the experiment could be poor fuel ventilation conditions in the initial stages of the fire in the experiment, prior to when the fire have created large enough holes in the fuel; also a phenomena which any of the models lack the capability to reproduce. Altogether, any, two or all of these three explanations may explain the grossly overestimation of CO for both models at the later stage of the fire.
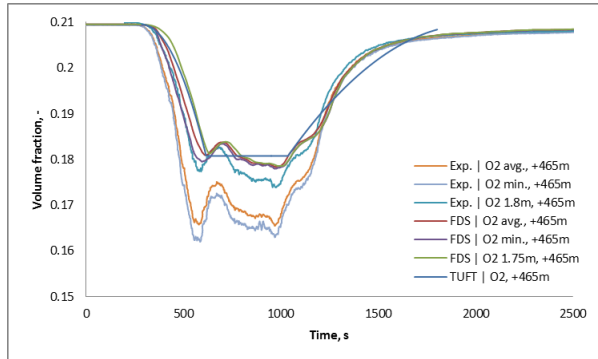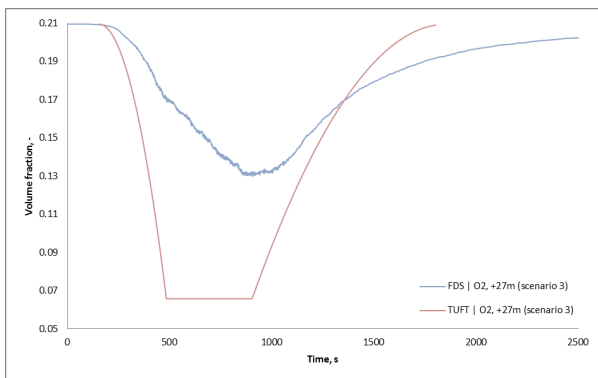

Figure 11. The volume fraction of oxygen measured 465 m downstream the fire source.
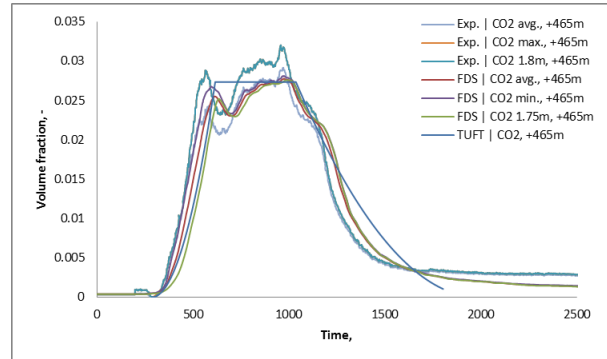
Figure 12. The volume fraction of carbon dioxide measured 465 m downstream the fire source.
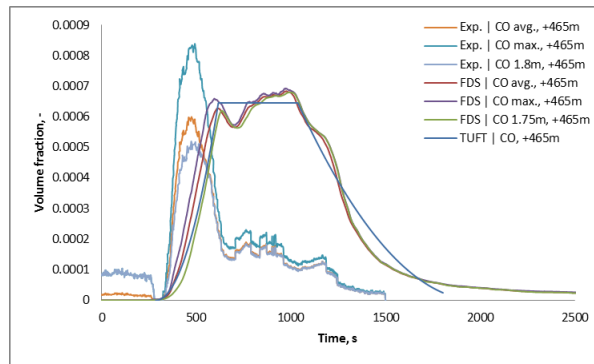
Figure 13. The volume fraction of carbon monoxide measured 465 m downstream the fire source.

### 3.1.4. Extinction Coefficient (Visibility)

As for the gas concentration measurements, described above, the visibility conditions were only measured at one position in the tunnel during the execution of the Runehamar experiment (465 m downstream the fire). Therefore, the measurements in FDS and TUFT are only presented for this location below. The measurements are termed according to an analogy similar to what is described above for the measurements of the gas temperature.

A trend, similar to what was described for the measurement of CO gas concentration, is identified in Figure 14. Up to ~500 s into the fire, the prediction of the extinction coefficient is fairly well represented by both FDS and TUFT. However, both models grossly overestimate the extinction coefficient thereafter. Probably, this has to do with the same phenomena as described in the previous section. During the time initial stage up to about 500-600 s it is also noted that FDS underestimate the extinction coefficient, this is most likely due to the average value that was used for the soot yield since time-dependant value cannot be specified.

The consequence of this is that both FDS and TUFT will underestimate the visibility conditions (visibility for reflecting signs is calculated by the following equation in TUFT: $2/C_s$, where C_s is the extinction coefficient, in FDS it is $3/C_s$ for light-reflecting signs and $8/C_s$ for light-emitting signs). If, for example, evacuation is modelled in this environment, the evacuating agents will move slower than what would be the case in reality. The effect, thus, causes the ending result to be over conservative.

12

For the comparison with the experiment, the maximum value of the mass optical density recorded from the experiment was selected to represent input to TUFT related to extinction coefficient calculations. As can be seen in Figure 14, this causes the extinction coefficient to be overestimated (hence, the visibility conditions underestimated). It is likely that the maximum measured value of the mass optical density was captured in the initial stages of the fire (due to reasons mentioned above), and therefore a better prediction of the visibility conditions is likely made with either a mean or an above-mean value of the mass optical density as input to TUFT.
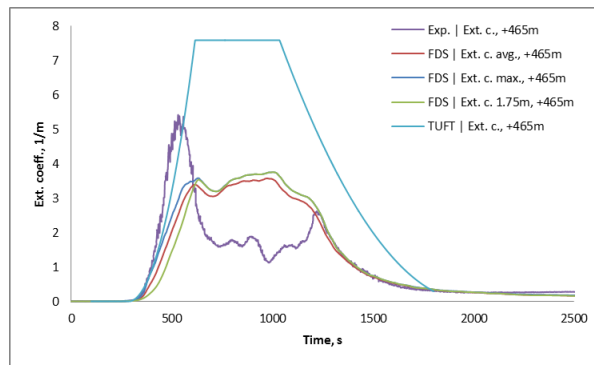
Figure 14. The extinction coefficient measured 465 m downstream the fire source.

3.1.5. Summary

Generally, FDS seem to better predict gas temperatures than TUFT, but both models have problems in areas close to the fire source. This is expected given the coarse grid size used in FDS and the lumped heat assumption that is being made in TUFT. In addition, TUFT is having problems farther downstream the fire where the cross sectional averaged gas temperature is under predicted. In this perspective, FDS is better and would probably be even better if a smaller grid size were used. A possible improvement of TUFT may be achieved by modifying the lumped heat-transfer coefficient, see chapter *TUFT and the Effect of the Lumped Heat Transfer Coefficient*.

In terms of prediction of gas concentrations, both FDS and TUFT performs reasonably well for O_2 and very well for CO_2. Earlier runs with FDS using a different chemical composition for the fuel yielded rather large deviations regarding both the O_2 and CO_2 concentrations, which indicated that this is a very sensitive parameter. Both models lack the ability to correctly predict the CO concentration over time with sufficient accuracy, and it is argued that this has to do with (1) the probable two-step reaction that happens in the experiment where CO reacts with oxygen to form CO_2 due to high temperatures, as seen in Figure 13, (2) that the plastic materials burnt off in the initial stages of the fire in the full-scale field study, or (3) changing ventilation conditions caused as a consequence of the fire in the fuel.

When it comes to the predictive capabilities of the extinction coefficient (and consequently the visibility conditions), TUFT display an overestimation while FDS show both an over- and underestimation. FDS also misses the initial peak due to the averaged soot-yield value that was used. The effect in the long run for TUFT (and in part FDS) in this specific case, for example when using the models to simulate evacuation processes in tunnels, is that the results later in the fire scenario probably will be over-conservative as, for example, the walking speed of the agents are reduced to a lower speed than what would be the case in a real fire. Therefore, it may not always be representative to choose the highest measured mass optical density value as an input to TUFT which was done in this report, but rather something in between the lowest and the highest (as done in FDS), if input is collected from an executed experiment as done in this case.

3.2. Part 2: Comparison between FDS and TUFT

Below the output of the comparative study is presented in graphs together with an ending summary. The information in the figures should be read together with the ending summary in order to facilitate the understanding of the information given. Only two scenarios are being displayed in the report (scenario 3 and 5) since they represent the general conclusions and also showcase deviations between the two models. The data from the rest of the scenarios can be seen in *Appendix B: Comparison between FDS and TUFT*.

3.2.1. Scenario 3 - Wind speed 0.5 m/s

Below, the simulation results related to scenario 3 for both models are presented. Data is presented for all parameters included above, i.e., gas temperature, gas concentrations and extinction coefficient.

3.2.1.1. Gas temperature
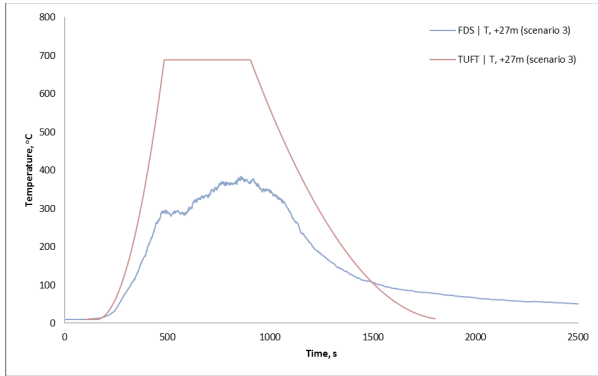
Figure 15. The gas temperature measured 27 m downstream the fire source.
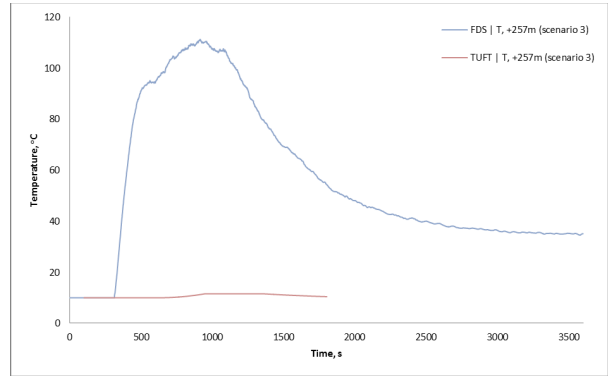
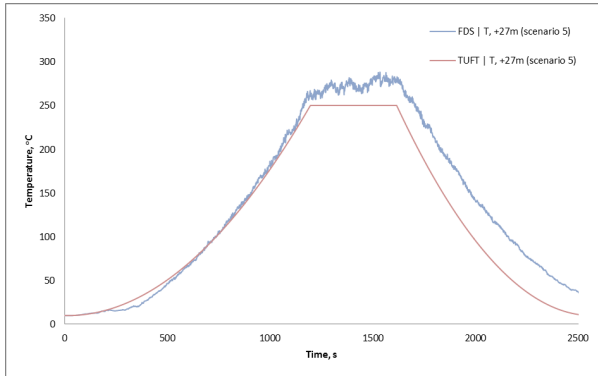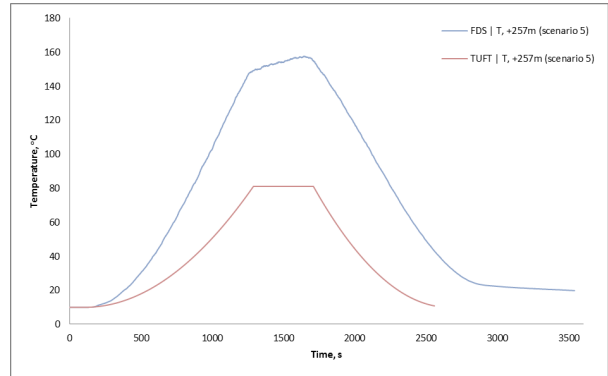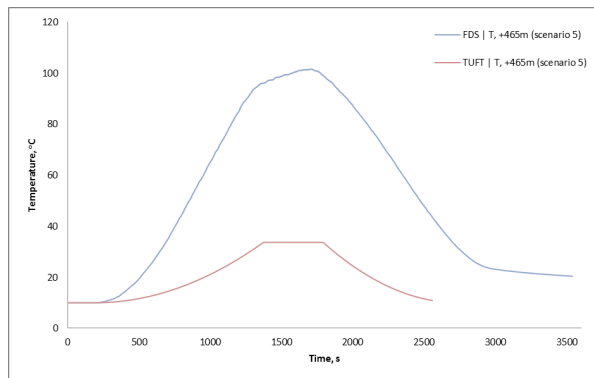Figure 16. The gas temperature measured 257 m downstream the fire source.
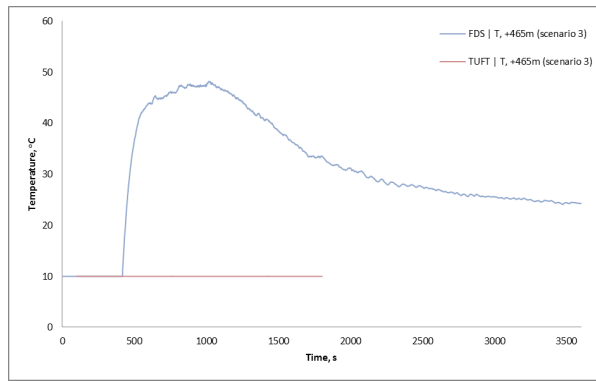
Figure 17 The gas temperature measured 465 m downstream the fire source.

3.2.1.2. Gas concentrations

Figure 18. The volume fraction of oxygen measured 27 m downstream the fire source.
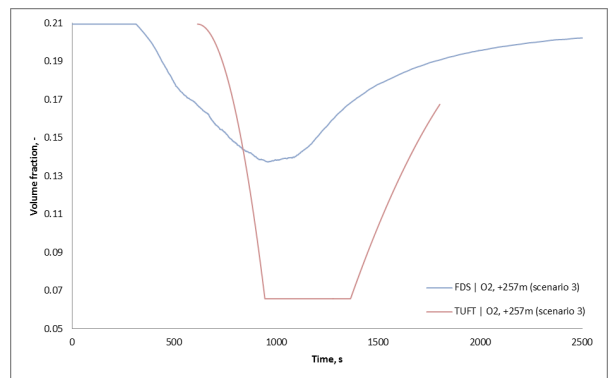
Figure 19. The volume fraction of oxygen 257 m downstream the fire source.

14
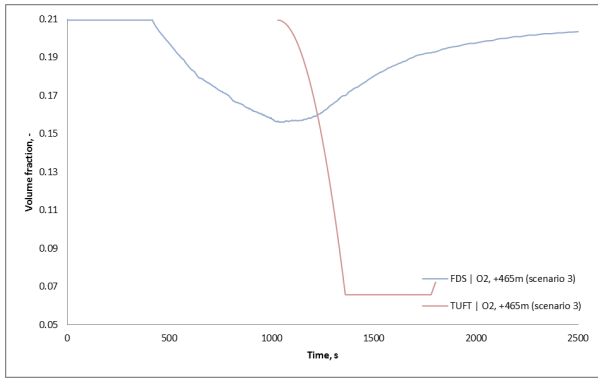
Figure 20. The volume fraction of oxygen 465 m downstream the fire source.
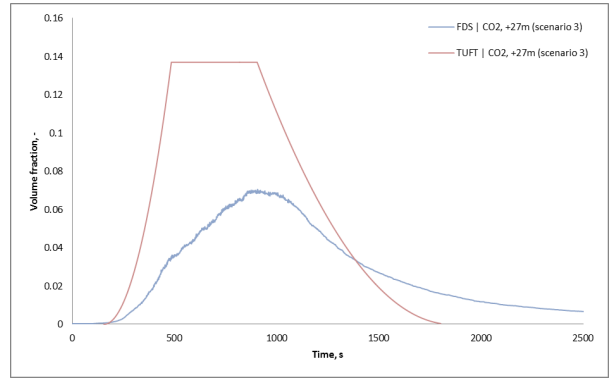
Figure 21. The volume fraction of carbon dioxide measured 27 m downstream the fire source.
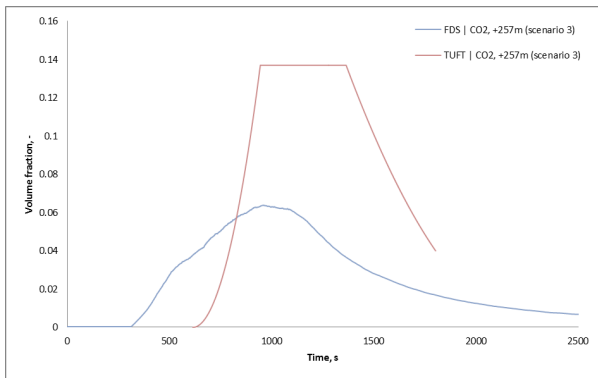
Figure 22. The volume fraction of carbon dioxide 257 m downstream the fire source.
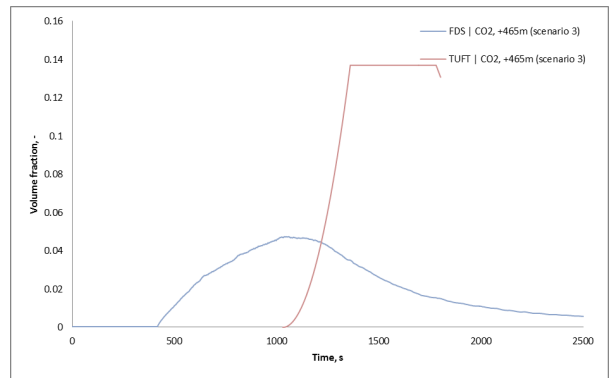
Figure 23. The volume fraction of carbon dioxide measured 465 m downstream the fire source.
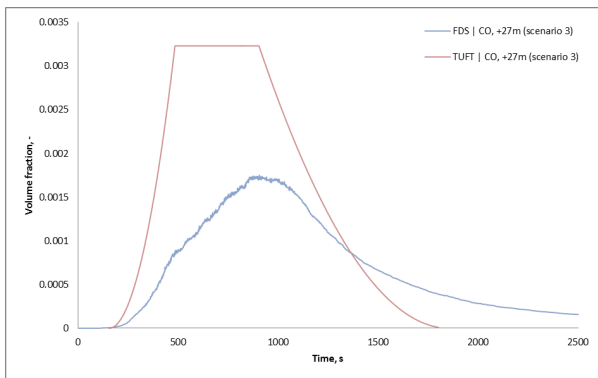
Figure 24. The volume fraction of carbon monoxide measured 27 m downstream the fire source.
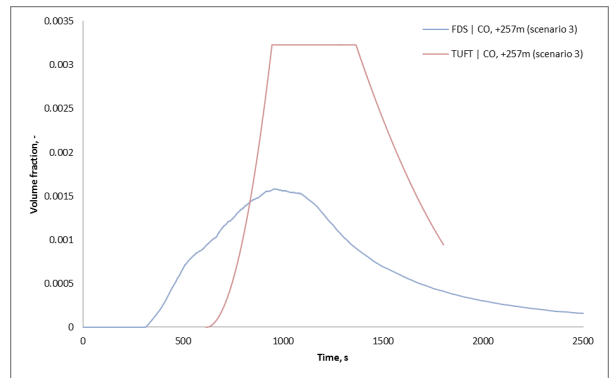
Figure 25. The volume fraction of carbon monoxide measured 257 m downstream the fire source.

15
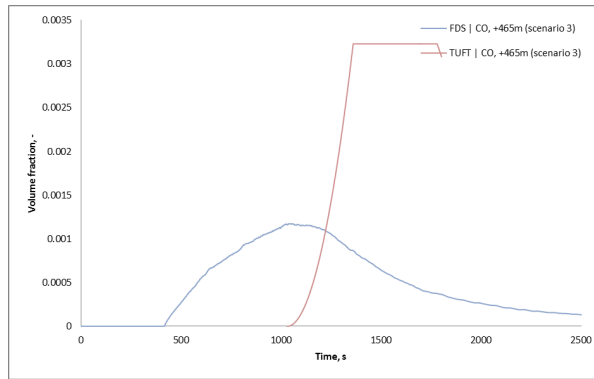
Figure 26. The volume fraction of carbon monoxide measured 465 m downstream the fire source.

3.2.2. Extinction Coefficient
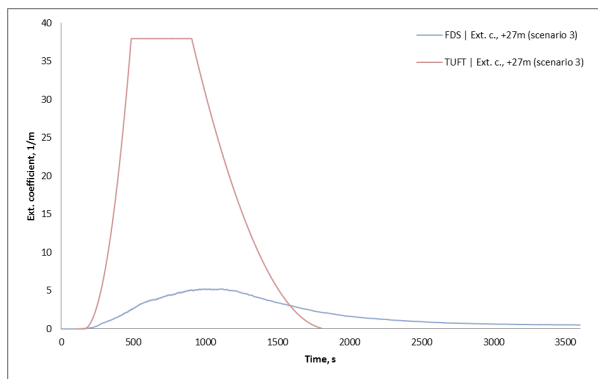
Figure 27. The extinction coefficient measured 27 m downstream the fire source.
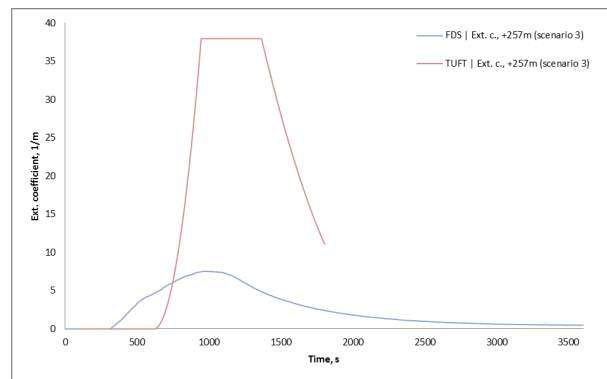
Figure 28. The extinction coefficient measured 257 m downstream the fire source.
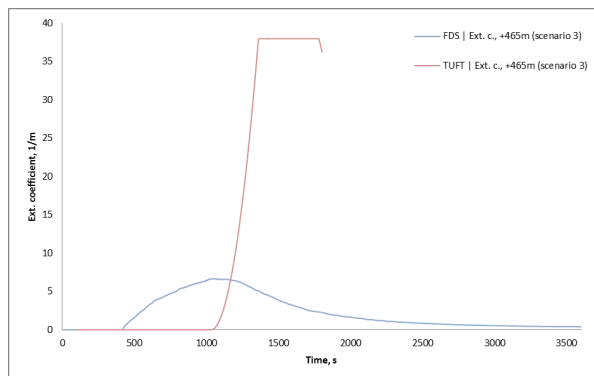
Figure 29 The extinction coefficient measured 465 m downstream the fire source.

16

3.3. Scenario 5 – HRR growth rate 0.047 kW/s^2

Below, the simulation results related to scenario 5 for both models are presented. Data is presented for all parameters included above, i.e., gas temperature, gas concentrations and extinction coefficient.

3.3.1. Gas temperature

Figure 30. The gas temperature measured 27 m downstream the fire source.

Figure 31. The gas temperature measured 257 m downstream the fire source.

Figure 32 The gas temperature measured 465 m downstream the fire source.

3.3.2. Gas concentrations
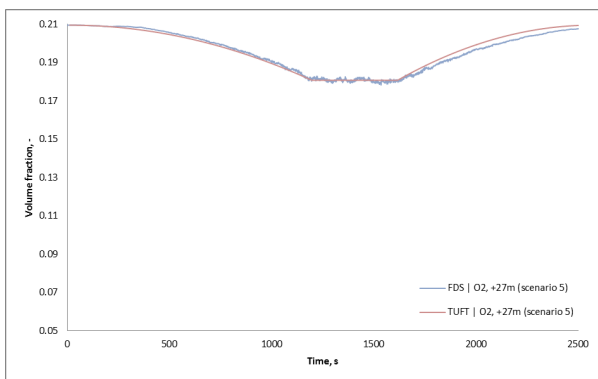
Figure 33. The volume fraction of oxygen measured 27 m downstream the fire source.
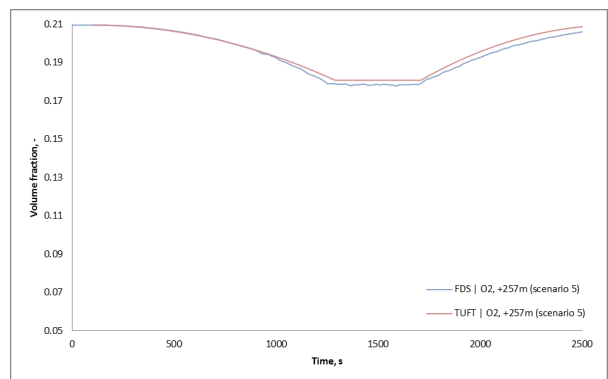
Figure 34. The volume fraction of oxygen 257 m downstream the fire source.
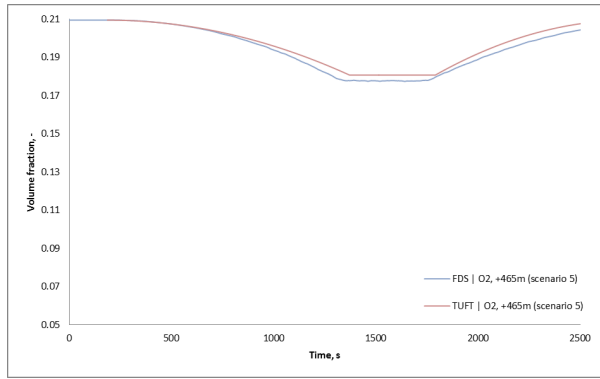
Figure 35. The volume fraction of oxygen 465 m downstream the fire source.
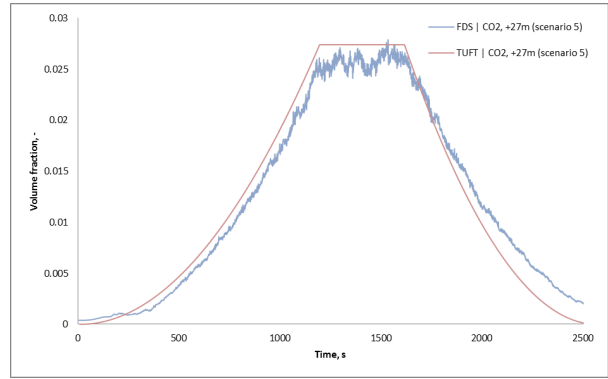
Figure 36. The volume fraction of carbon dioxide measured 27 m downstream the fire source.
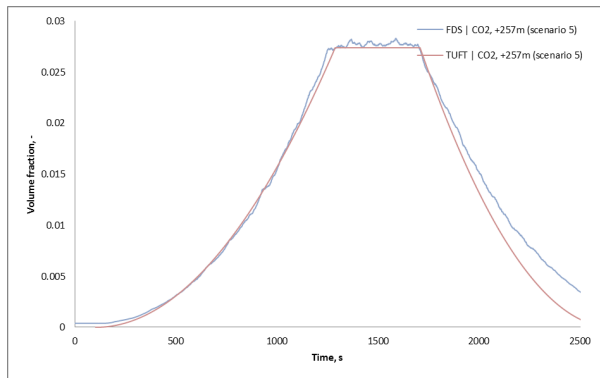
Figure 37. The volume fraction of carbon dioxide 257 m downstream the fire source.
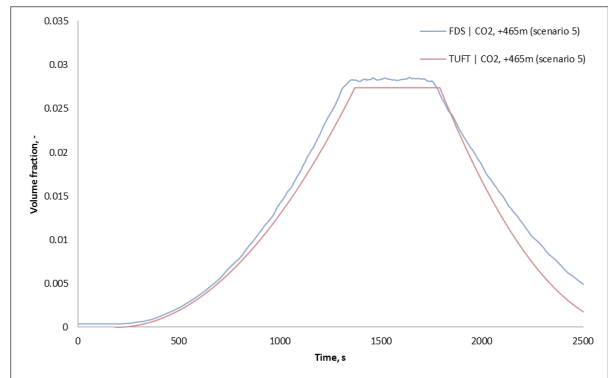
Figure 38. The volume fraction of carbon dioxide measured 465 m downstream the fire source.
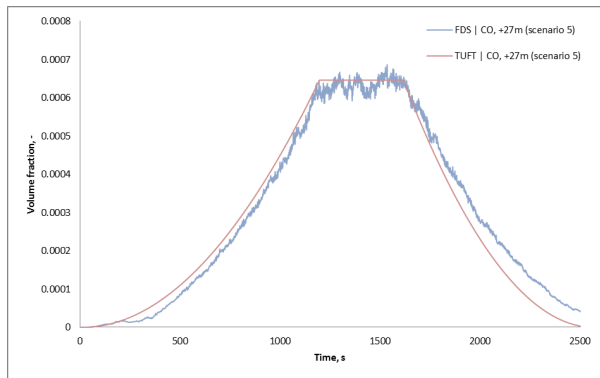
Figure 39. The volume fraction of carbon monoxide measured 27 m downstream the fire source.
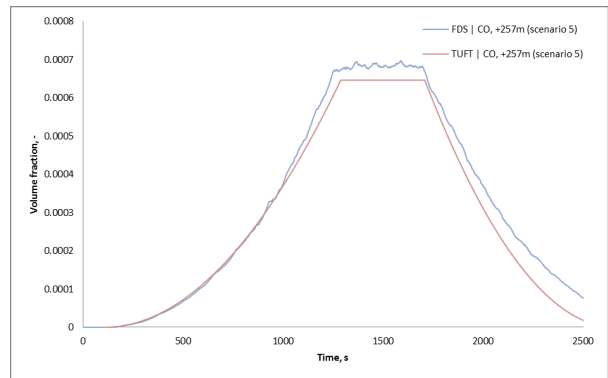
Figure 40. The volume fraction of carbon monoxide measured 257 m downstream the fire source.
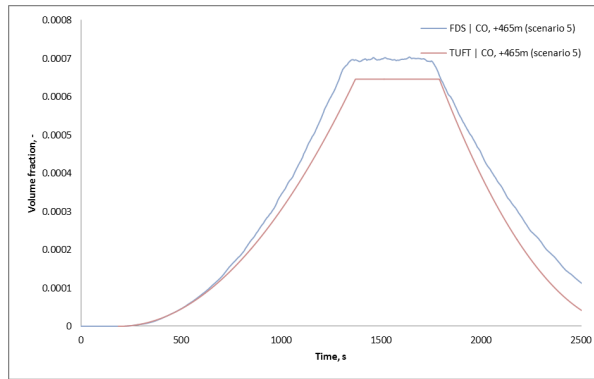
Figure 41. The volume fraction of carbon monoxide measured 465 m downstream the fire source.

3.3.3. Extinction Coefficient
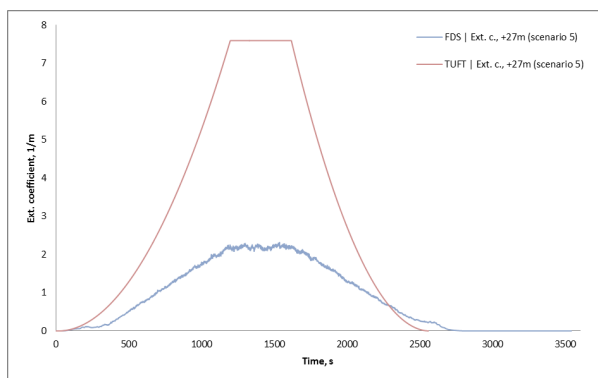
Figure 42. The extinction coefficient measured 27 m downstream the fire source.
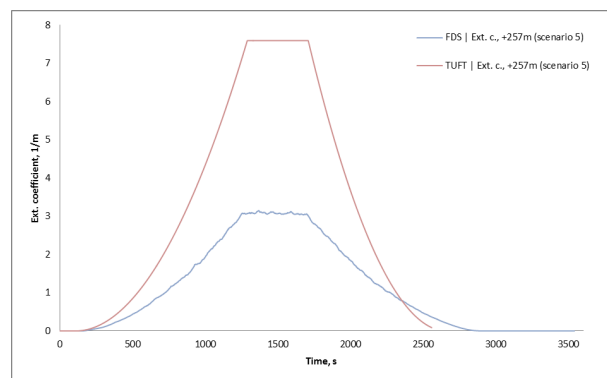
Figure 43. The extinction coefficient measured 257 m downstream the fire source.
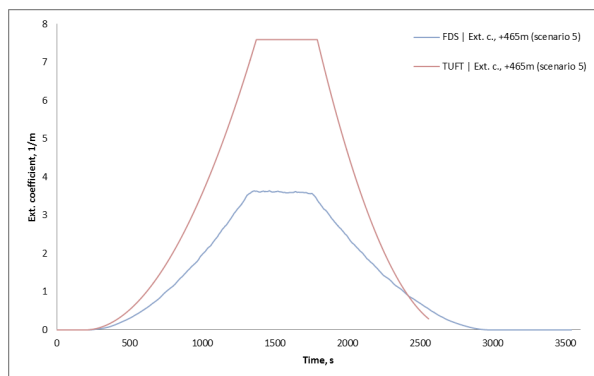
Figure 44 The extinction coefficient measured 465 m downstream the fire source.

3.3.4. Summary

Above, two representative scenarios (out of a total of six) has been selected to illustrate the most interesting observations in the comparison between FDS and TUFT and their corresponding representation of gas temperature, gas concentrations and extinction coefficient for a tunnel fire. Below, a summary discussion related to the findings are presented. Note, however, that the discussion is based on the results of all six scenarios and not only the two illustrated above. Therefore, the interested reader should also consult Appendix B: Comparison between FDS and TUFT when analysing the data.

Regarding the gas temperature, once again it can be seen that TUFT and FDS predict roughly the same temperature close to the fire (with one exception, discussed in the next paragraph) but further down the

tunnel TUFT probably loses too much heat to the surrounding walls and under-predicts the gas temperatures. This discrepancy has been acknowledged and is discussed further in the chapter *TUFT and the Effect of the Lumped Heat Transfer Coefficient.*

Another major discrepancy of the temperature can be seen when looking at the scenario with the lower tunnel velocity (0.5 m/s). Both the magnitude and temporal resolution have very large differences, with TUFT predicting higher temperatures and slower transport in the tunnel. This is probably due to the fact that TUFT only uses the prescribed tunnel flow to predict the gas temperature (heating of a gas volume) and transport time (distance divided by velocity) and cannot take into account the buoyancy and plume momentum that is caused by the fire itself, which FDS can. When the tunnel velocity gets too low the driving forces created by the fire becomes dominant and the TUFT model becomes invalid, hence the large difference between the two models.

Regarding the species concentrations the results from FDS and TUFT are in very good agreement with each other both close to the fire and further downstream in the tunnel, except for the scenario with the lower tunnel velocity (0.5 m/s). The same phenomena the was discussed in the paragraph above seems to be valid here, when the tunnel velocity gets too low the driving forces created by the fire becomes dominant and the TUFT model becomes invalid, hence the large difference between the two models.

The overall good species concentration agreement was somewhat expected due to the fact that both models used the same yields for all three species of interest. Even though the CO_2-yield cannot be explicitly given in FDS it is possible to match the two with some balancing of the chemical reaction that takes place in FDS. Initial simulations using the wrong effective CO_2-yield resulted in rather large discrepancies compared to TUFT, which showcases the sensitivity of these parameters. Since the CO_2 production was wrong the O_2 consumption was wrong and in the end the O_2 concentration also was wrong. The CO-yield however is always explicitly stated and did not display the same problems.

Regarding the extinction coefficient there is a very large discrepancy between the two models which is most likely due to the large difference in the source terms given in each model. FDS calculates the extinction coefficient using the local soot concentration, and is therefore controlled by the soot yield, while TUFT uses the mass optical density. Calculating the used soot yield (0.02) to a mass optical density gives an approximate value of 75 m^2/kg, which vastly differs from the value of 120 m^2/kg used in TUFT by a factor of about 1.6. This explains the large difference between the models to some degree, but there are still even larger relative differences and also temporal mismatches, which is the most evident in the scenario with the slower tunnel flow velocity. This can once again probably be explained by that the driving forces that are created by the fire becomes dominant relative the tunnel flow velocity and the TUFT model is incapable of predicting this effect.

4. Evacuation

In relation to the results presented above, some links to evacuation and evacuation modelling has been done. As an example, the under estimation of visibility in both FDS and TUFT may cause agents to walk slower than what is actually the case in real fires. This may, in turn, cause FED estimations to be over conservative, as the evacuees are believed to spend longer times in the fire affected tunnel environments than what is actually the case.

In order to illustrate the effects of a fire identical to the Runehamar T4-fire, an evacuation analysis has been performed using TUFT. In the analysis, four people are assumed trapped in a road tunnel with the same physical dimensions as described in Table 1, with the addition that the tunnel has emergency exits placed each 150 m. Person 1 and 2 are assumed to be trapped at a position 100 m downstream the fire source, with 60 s recognition time (which they spend in their vehicles) and 120 s response time. The difference between the persons is that Person 1 evacuates towards the tunnel portal/exit, and that Person 2 evacuates to the closest emergency exit downstream (1200 m). Modelling of walking speeds are done according to (Fridolf et al., 2013), and the accumulated fractional incapacitating dose (FID) is evaluated according to the FED concept (Purser, 2008, 2009). Evaluations are done for each time step, which is every second. An additional two persons (Person 3 and 4) are also included. In contrast to Person 1 and 2, they start evacuating from a position 200 m downstream the fire. Person 3 evacuates towards the tunnel portal, whereas Person 4 evacuates towards the closest emergency exit downstream (1350 m).

For this particular fire, it is clear the heat will play a dominant role in terms of survival, especially for the people that are assumed to move toward the tunnel portal downstream the fire. As can be seen in Figure 45, an incapacitating dose of heat is reached for Person 1 after about 450 s and for Person 3 after about 700 s. Assuming then that they stop at their positions, they continue to be affected by the heat until a lethal dose is acquired after about 610 s and 1050 s respectively. Figure 46 furthermore describes the uptake of asphyxiants, and for Person 1 and 3 the intake is reduced when they are incapacitated due to an assumed lower respiratory rate (an assumption made in TUFT, according to (Purser, 2008)). Person 2 and 4 do, however, survive the fire with little affect from both heat and asphyxiants. Naturally, this has to do with the fact that they reach a safe place (the emergency exit) after 370 s and 400 s respectively.

Each Persons movement in the tunnel can be tracked in Figure 47, where the person's position is described as a function of the time. As can be seen, all four persons move relative quick initially, but as the fire grows and the smoke gets denser, their walking speeds are reduced, resulting in a slower movement.
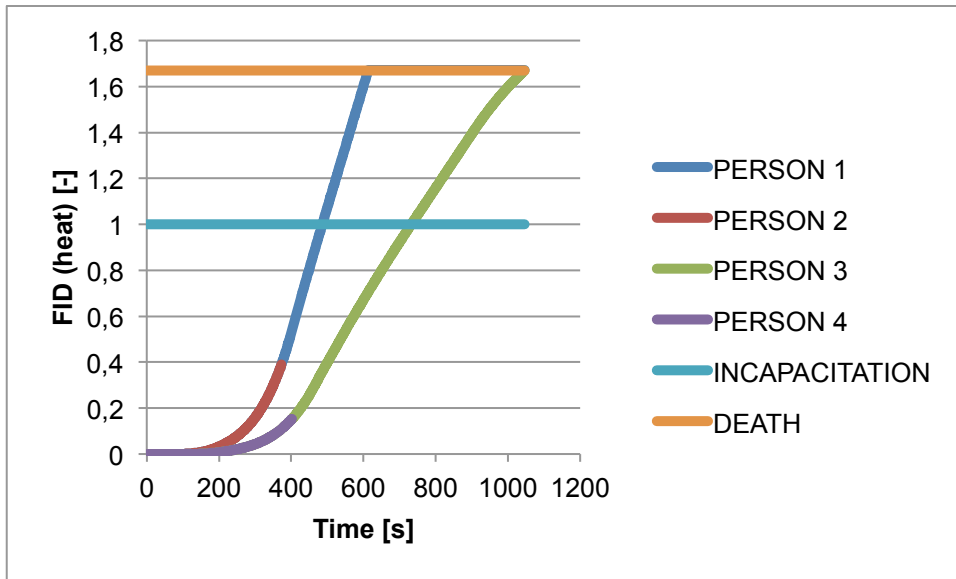
Figure 45. Accumulated fractional incapacitating dose of heat. For reference, the accumulated dose representing incapacitation as well as death is illustrated. Person 1 and 3 do not survive, 2 and 4 do due to the fact that they evacuated toward the closest emergency exit.
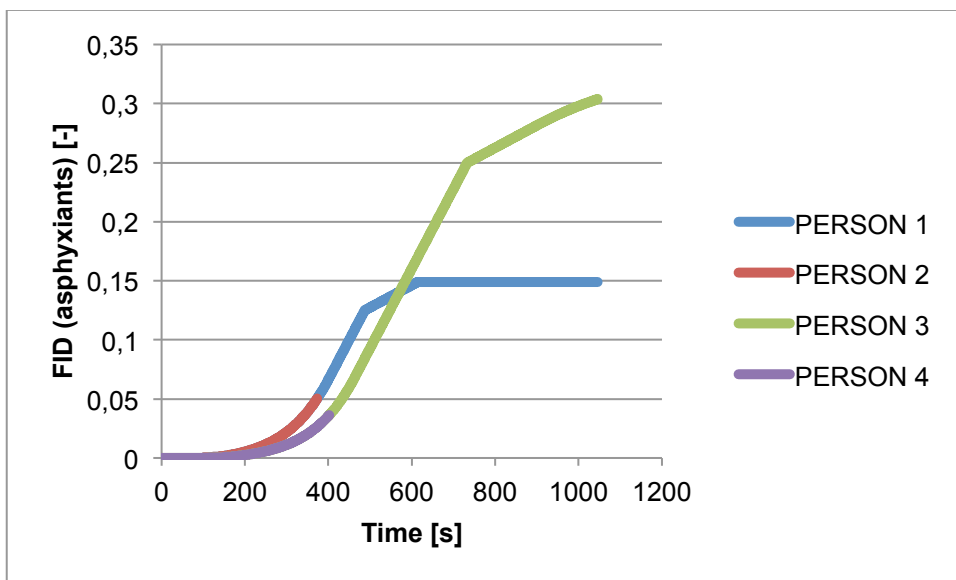
Figure 46. Accumulated fractional incapacitating dose of asphyxiants.
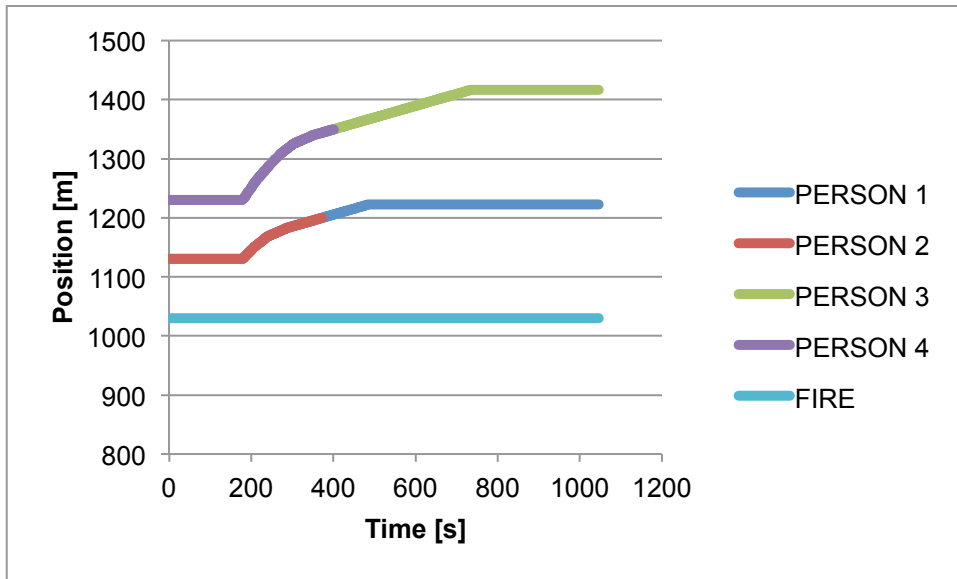
Figure 47. The position of each person as a function of time during their evacuations. The position of the fire source is included for reference.

5. TUFT and the Effect of the Lumped Heat Transfer Coefficient

A conclusion of the results presented above was that TUFT predicted much lower cross sectional averaged gas temperatures than what was measured in the full-scale experiment. In the light of this, the impact of the lumped heat-transfer coefficient (including both convective and radiative heat losses to the tunnel walls) was discussed. By lowering the value from 0.03 to 0.02, a better prediction is achieved, which clearly is illustrated in Figure 48 – Figure 56. Thus, a more conservative calculation seems to be achieved if a lower value of the lumped heat transfer coefficient is chosen prior to the analysis. It is therefore recommended.

Another way to achieve the same effect, e.g., to reduce the heat transfer to the tunnel walls, would be to model heat transfer differently. As is done according to Equation 1, the heat transfer is calculated in relation to the tunnel perimeter. According to the assumptions of the underlying bulk equations, this is of course right, but when put in the context of a real fire it is relevant to ask where the actual heat transfer will take place. Most likely, this is through the tunnel ceiling and uppermost parts of the tunnel walls. Thus, an alternative to lowering the value of the lumped heat transfer coefficient could be to assume that heat transfer is only taking place on, e.g., half of the tunnel perimeter. The effects of this has, however, not been studied in any greater detail.
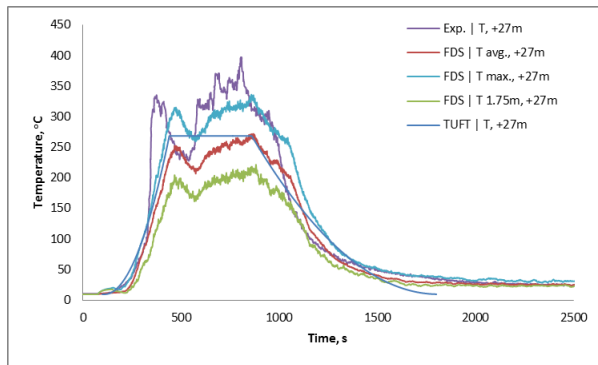
Figure 48. The gas temperature measured 27 m downstream the fire source.
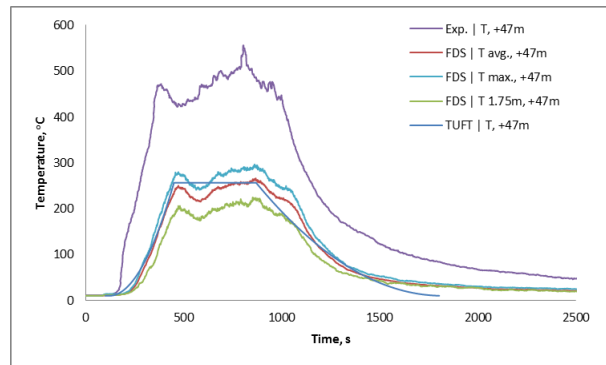
Figure 49. The gas temperature measured 47 m downstream the fire source.
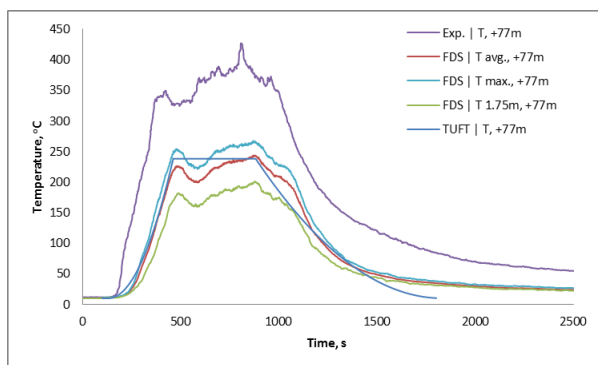
Figure 50. The gas temperature measured 77 m downstream the fire source.
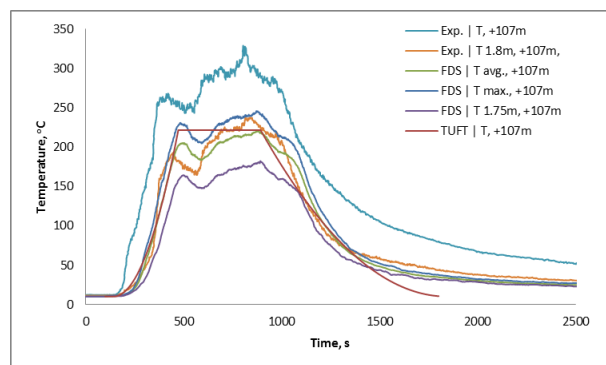
Figure 51. The gas temperature measured 107 m downstream the fire source.
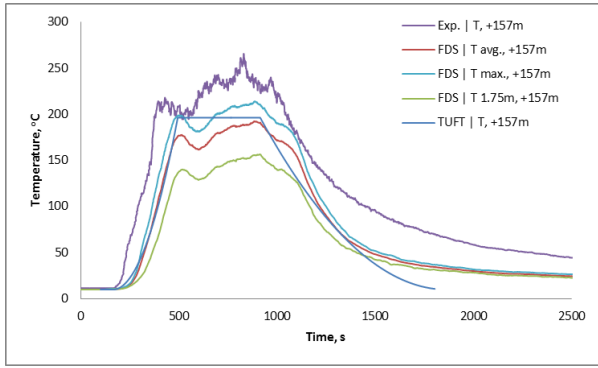
Figure 52. The gas temperature measured 157 m downstream the fire source.
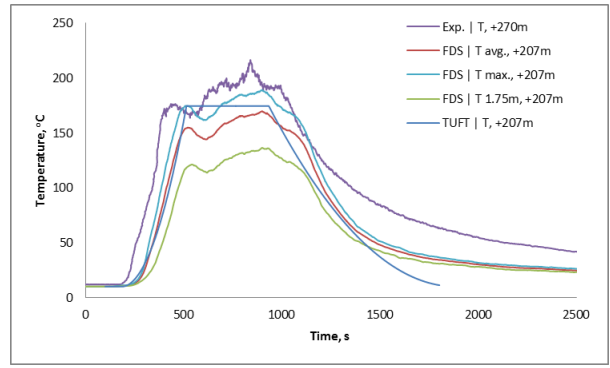
Figure 53. The gas temperature measured 207 m downstream the fire source.
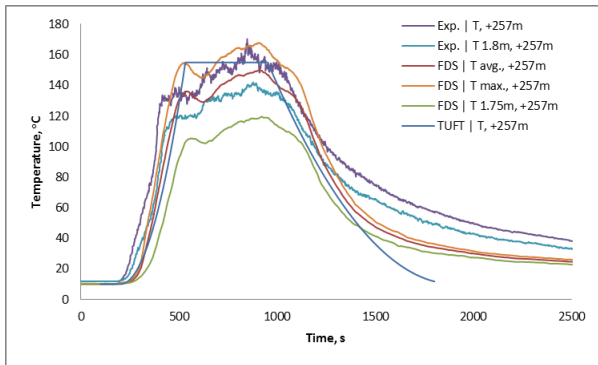
Figure 54. The gas temperature measured 257 m downstream the fire source.
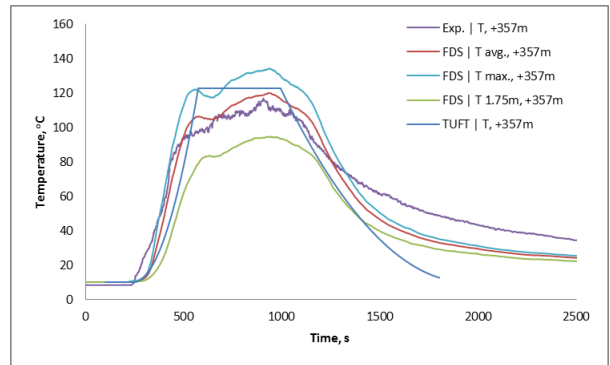
Figure 55. The gas temperature measured 357 m downstream the fire source.
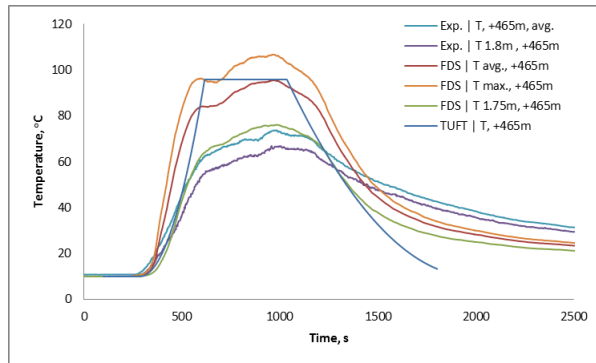
Figure 56. The gas temperature measured 465 m downstream the fire source.

26

6. Conclusions

In this report, the capability of reproducing tunnel fires of two different fire dynamic models (FDS and TUFT) have been examined partly by comparing modelling results with a real full-scale field fire experiment and partly by comparing the simulation results of both models with each other for six pre-defined scenarios. In the comparison with the full-scale field experiment, it is revealed that although FDS represents a much more advanced model, the capability of reproducing the experiment measurements is not significantly better than TUFT. Some differences in terms of, e.g., temperature was found, but a suggestion was also made on how these differences could be reduced by (for example) lowering the lumped heat transfer coefficient in TUFT, and thus getting a better agreement with both the full-scale field experiment and TUFT.

In the end, it is obvious that the input to any of the two models included in the report is extremely important and will have a large effect on the output produced. In turn, this may for example affect assessments of different evacuation scenarios, as these simulations uses information from the fire dynamics calculations. As an example, it was above shown that by selecting the "worst case" value of the mass optical density as input to TUFT, the extinction coefficient was grossly overestimated (and consequently the visibility underestimated). In turn, this will affect agents to walk slower in an evacuation simulation, which may cause over conservative predictions in the end as both FED calculations and evacuation times are overestimated.

In summary, the most important conclusions of this report are reproduced below:

- In the comparison with the full-scale field experiment, both FDS and TUFT seem to under predict the gas temperature close to the fire source (~100 m downstream the fire). Better predictions are made from approximately 150 m downstream the fire, and further down.
- In TUFT, a one-dimensional bulk model to estimate the cross-sectional gas-temperature is used. This model uses a lumped heat transfer coefficient for both radiative and convective heat transfer to the walls, and a value of .03 was assumed in the original model. This caused the model to under predict the temperature compared to the full-scale field experiment, and the difference became even greater the farther away from the fire source the prediction was made. Lowering the lumped heat transfer coefficient to .02 demonstrated a much better agreement with both the full-scale field experiment measurements and FDS. It is therefore recommended that this value be used instead.
- Gas concentration predictions of O_2 corresponded well to the measurements done at head height (1.8 m) in the full-scale field experiment. Predictions of CO_2 were very good, however, the predictions of CO was poor (both models grossly over predicted the concentration). Three possible explanations of this have been discussed in the report, and the affect on evacuation simulations including FED calculations should be acknowledged (evacuation simulations including FED calculations will reach incapacitation/death levels much faster than what may be the case in real fires due to the high concentrations).
- Both models perform poorly in terms of predicting visibility conditions. The link to the prediction of CO is obvious, and the poor capability will in turn affect evacuation simulations performed in any of the models conservatively.
- The mass optical density is identified as a very sensitive parameter in TUFT in terms of predicting visibility conditions. In the comparison with the full-scale field experiment, the highest recorded value from the experiment was selected as input to TUFT. This caused gross over predictions of the extinction coefficient, and in turn under predictions of the visibility.
- In the comparative study between FDS and TUFT, some of the differences seen in the comparison with the full-scale field experiment were identified again (e.g., differences in prediction of extinction coefficient). Apart from that, the models produced roughly the same results with one exception: With very low wind speeds, TUFT seems incapable of predicting most fire dynamic parameters. This is related to the inability to model buoyancy and plume momentum, which is captured in FDS but not TUFT, and the results suggest that TUFT is not

used in fire scenarios involving no mechanical ventilation (or in scenarios where the wind speed is very low).

7. References

Bergqvist, A. (2000). Branden i Tauerntunneln. Karlstad: Statens räddningsverk.

Bergqvist, A. (2001). Rapport ifrån besöket vid brandplatsen i Kaprun, Österrike. Stockholm: Stockholms Brandförsvar.

Carvel, R., & Marlair, G. (2011). A history of fire incidents in tunnels. In A. Beard & R. Carvel (Eds.), *Handbook of Tunnel Fire Safety* (Second ed., pp. 3-23). London, UK: ICE Publishing.

Dix, A. (2010). Tunnel Fire Safety in Australasia. In A. Lönnermark & H. Ingason (Eds.), *Proceedings from the Fourth International Symposium on Tunnel Safety and Security, Frankfurt am Main, Germany, March 17-19, 2010* (pp. 69-79). Borås, Sweden: SP Technical Research Institute of Sweden.

Donald, I., & Canter, D. (1990). Behavioural Aspects of the King's Cross Disaster. In D. Canter (Ed.), *Fires and Human Behaviour* (2 ed., pp. 15-30). London: David Fulton.

Duffé, Pierre, & Marec, Michel. (1999). Task Force for Technical Investigation of the 24 March 1999 Fire in the Mont Blanc Vehicular Tunnel. (Vol. 2010): Minister of the Interior - Ministry of Equipment, Transportation and Housing.

Fennell, Desmond. (1988). *Investigation into the King's Cross Underground Fire.* London: The Department of Transport.

Fermaud, C., Jenne, P., & Müller, W. (1995). *Fire in a Commuter Train - Rescue Procedures as Perceived by Passengers.* Paper presented at the second International Conference on Safety in Road and Rail Tunnels, Granada, Spain.

Fridolf, K., Andrée, K., Nilsson, D., & Frantzich, H. (2013). The Impact of Smoke on Walking Speed. *Fire and Materials.* doi: 10.1002/fam.2217

Fridolf, K., & Frantzich, H. (2014). *Fire Protection of Underground Transportation Systems: A Decision Support Tool for Designers and Rescue Services.* Paper presented at the SFPE 10th International Conference on Performance-Based Codes and Fire Safety Design Methods, Brisbane, Australia.

Ingason, H. (2012). Fire dynamics in tunnels. In A. Beard & R. Carvel (Eds.), *Handbook of Tunnel Fire Safety* (Second ed., pp. 273-307). London, UK: ICE Publishing.

Ingason, H., & Lönnermark, A. (2012). Heat release rates in tunnel fires: a summary. In A. Beard & R. Carvel (Eds.), *Handbook of Tunnel Fire Safety* (Second ed., pp. 309-328). London, UK: ICE Publishing.

Ingason, H., Lönnermark, A., & Ying Zhen, Li. (2011). Runehamar Tunnel Fire Tests. Borås, Sweden: SP Technical Research Institute of Sweden.

Larsson, Sara. (2004). Tunnelolyckan i Kaprun 2000 [Tunnel Accident in Kaprun 2000] (pp. 58). Stockholm: Försvarshögskolan [Swedish National Defence College].

Purser, D. (2008). Assessment of Hazards to Occupants from Smoke, Toxic Gases, and Heat. In P. J. DiNenno (Ed.), *The SFPE Hanbook of Fire Protection Engineering* (Fourth ed., pp. 2-96 - 92-193). Quincy, USA: National Fire Protection Association.

Purser, D. (2009). Hazards from toxicity and heat in fires. Hartford, UK: Hartford Environmental Research.

Rohlén, P., & Wahlström, B. (1996). Tunnelbaneolyckan i Baku, Azerbaijan 28 oktober 1995 [The Subway Accident in Baku, Azerbaijan, 28 October 1995]. Karlstad: Statens räddningsverk [Swedish Rescue Services Agency].

Schupfer, Hupert. (2001, April 4). *Fire disaster in the tunnel of the Kitzsteinhorn funicular in Kaprun on 11 Nov. 2000.* Paper presented at the fourth International Conference on Safety in Road and Rail tunnels, Madrid, Spain.

Statens Haverikommission. (2009). Brand i tunneltåg vid Rinkeby station, AB län, den 16 maj 2005. Stockholm: Swedish Accident Investigation Board.

Voeltzel, A. (2002). Compared analysis of the Mont Blanc Tunnel and the Tauern Tunnel fires *PIARC WG6* (pp. 1-11).

von Hall G. (2000, December 12). Tunneln blev en dödsfälla, *Svenska Dagbladet.*

Wildt-Persson, Bertil. (1989). Stora olyckor - Branden vid King's Cross tunnelbanestation i London. Karlstad: Statens räddningsverk.

Appendix A: Deriving Input Data to the Computer Models

Heat of combustion

A mass weighted heat of combustion was calculated using the specifications given in the Runehamar report [Table 2.1 and table 4.1 in Ingason et al., 2011], in part reproduced in Table 4. To confirm that this was representative the total energy and mass was calculated backwards using the heat release rate data.

Table 4 Specifications of the fire load that was used to calculate a mass averaged heat of combustion.

Description of fire load	Total weight [kg]	Theoretical calorific energy [GJ]
600 corrugated paper cartons with interiors (600 x 400 x 500 mm; L x W x H) and 15 % of total mass of unexpanded polystyrene (PS) cups (18000 cups) and 40 wood pallets (1200 x 1000 x 150 mm); 10 m² polyester tarpaulin	2849	62

Using 100% combustion efficiency and a calculated mass weighted heat of combustion of 22.2 MJ/kg the energy released did not reach the total energy given in the report (62 GJ). Compensating this using a combustion efficiency of 90% gave very good fit to the total energy given and was therefore used. Calculating the total burned mass from the energy released also yielded a very good fit to the value given in the report (2849 kg).
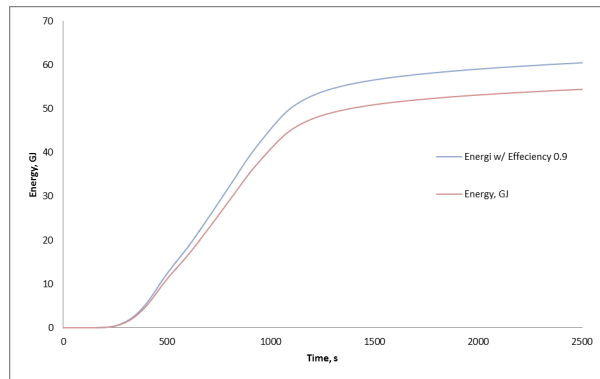
Figure 57 Total energy released from the fire source over time.
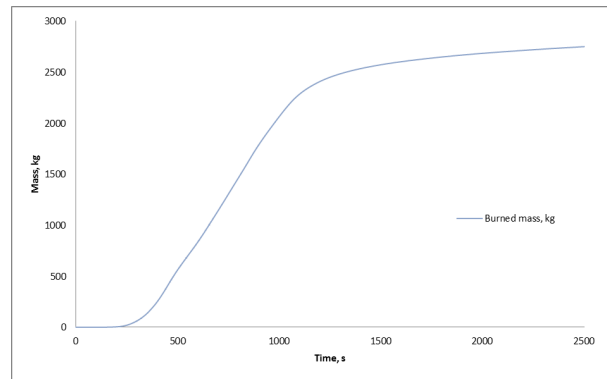
Figure 58 Total burned mass from the fire source over time.

CO2- and CO-yields

The CO2- and CO-yields were calculated each given time using the following equation:

$$\frac{\sum_{0}^{t}\left(\frac{M_i}{M_{air}} \cdot c(t)_{i,average}\right) \cdot \dot{m}(t)_{tunnel}}{\sum_{0}^{t} \dot{m}(t)_{fire}}$$

Where M_i is the molar mass of the species of interest, $c(t)_{i,average}$ is the average volume concentration of the species of interest, $\dot{m}(t)_{tunnel}$ is the mass flow in the tunnel and $\dot{m}(t)_{fire}$ is the mass loss rate from

the fire source. This assumed lumped gas transport and used average gas temperatures to estimate the mass flow in the tunnel. It also assumed that the combustion gases could be treated as heated air. The following graphs show the calculated values for CO_2 and CO:
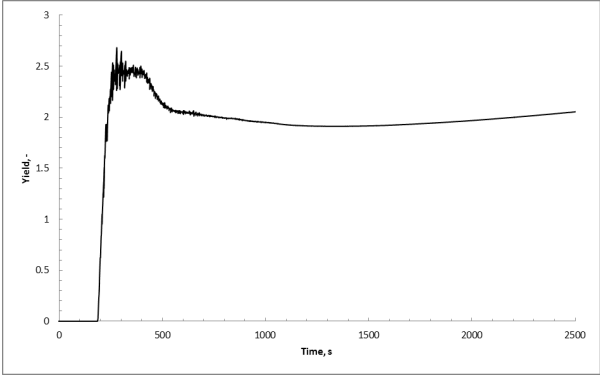
Figure 59 CO_2-yield as a function of time derived from the Runehamar T4 test.
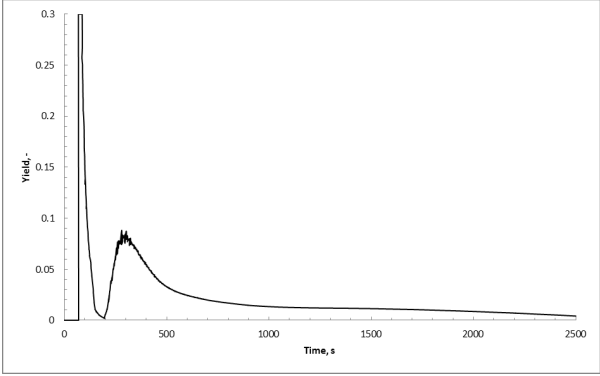
Figure 60 CO-yield as a function of time derived from the Runehamar T4 test.

Since neither of the computer models could use time dependant yields the CO_2-yield was approximated to 2.0 and the CO-yield was set to 0.03. Since the CO_2-yield could not specifically be set in FDS, a mix of wood and polystyrene (85 mass-% wood, 15 mass-% polystyrene) was chosen to be representative of the bulk fire chemical composition. This resulted in a CO_2-yield of 2.01 which was almost the same as the one used in TUFT (2.00)

Appendix B: Comparison between FDS and TUFT

This appendix contains the remaining graphs of the comparison between FDS and TUFT for the scenarios that were not presented in the report due to space limitations. As a reminder to the reader the scenario numbers are yet again listed below:

Scenario	Modification
1	Width = 2 m
2	Height = 3 m
3	Wind speed = 0.5 m/s
4	Wind speed = 4 m/s
5	Growth rate = 0.047 kW/s^2
6	Growth rate = 0.19 kW/s^2

As before all the FDS values are values averaged over the full tunnel height to get a similar output value compared to TUFT.

Scenario 1 – Tunnel width 2 meters

Gas temperature
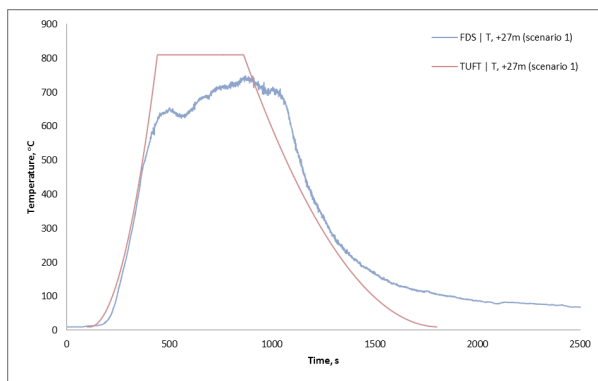
Figure 61. The gas temperature measured 27 m downstream the fire source.
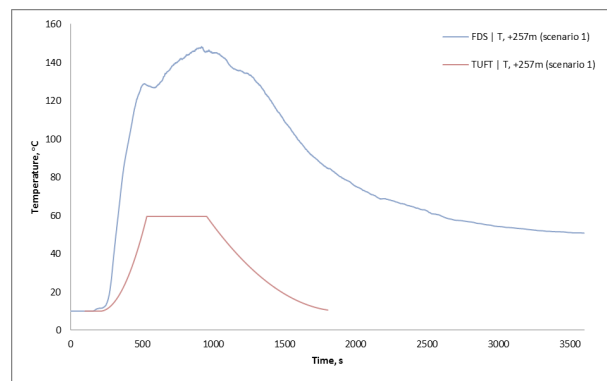
Figure 62. The gas temperature measured 257 m downstream the fire source.
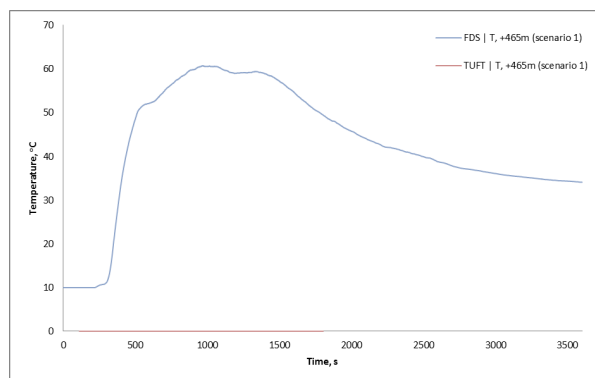
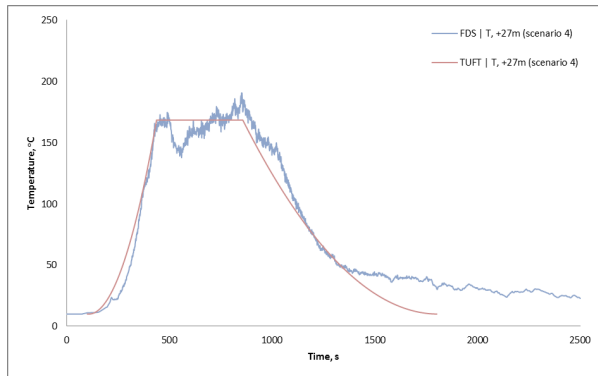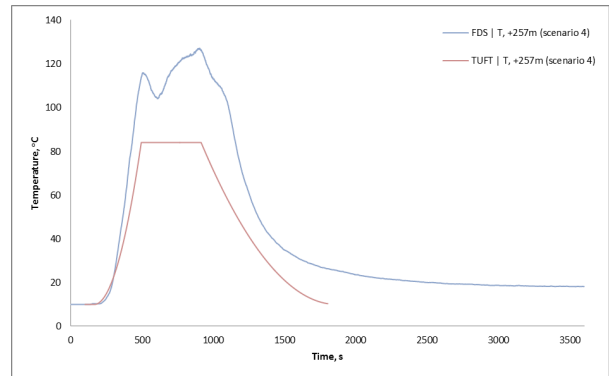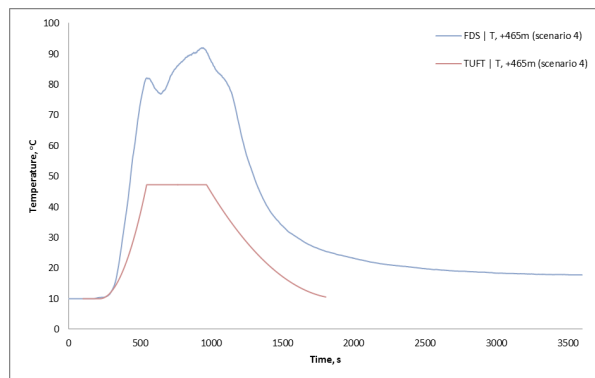Figure 63 The gas temperature measured 465 m downstream the fire source.
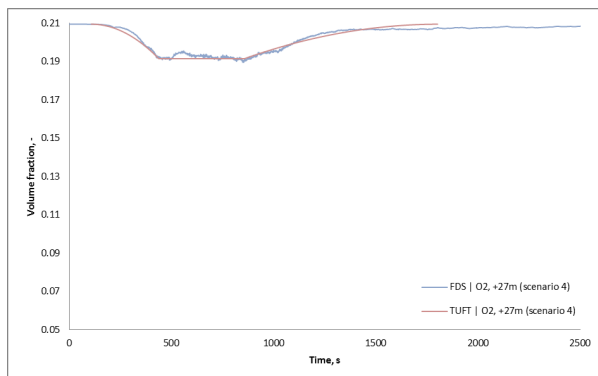
Gas concentrations
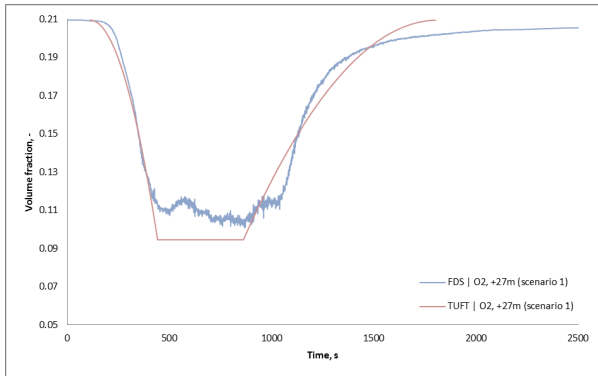
Figure 64. The volume fraction of oxygen measured 27 m downstream the fire source.
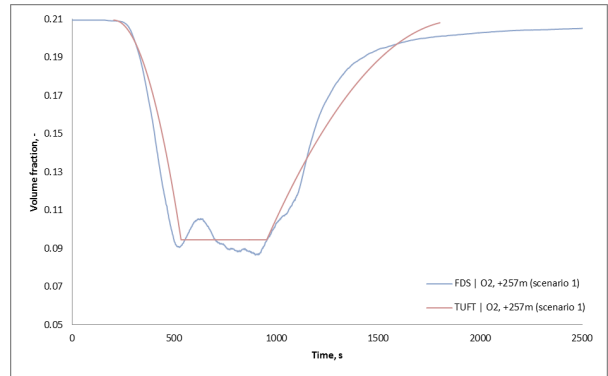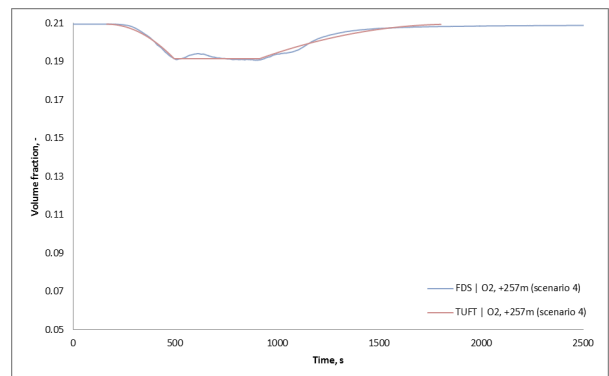

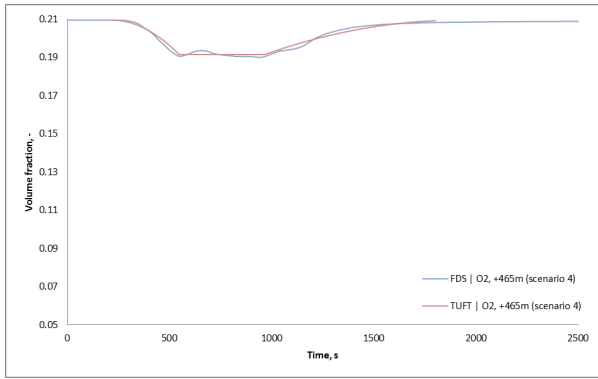Figure 65. The volume fraction of oxygen 257 m downstream the fire source.
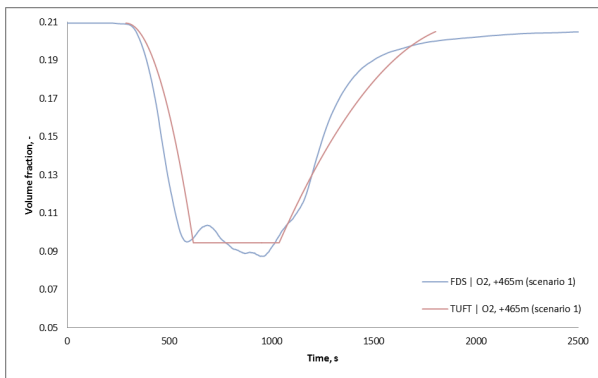
Figure 66. The volume fraction of oxygen 465 m downstream the fire source.
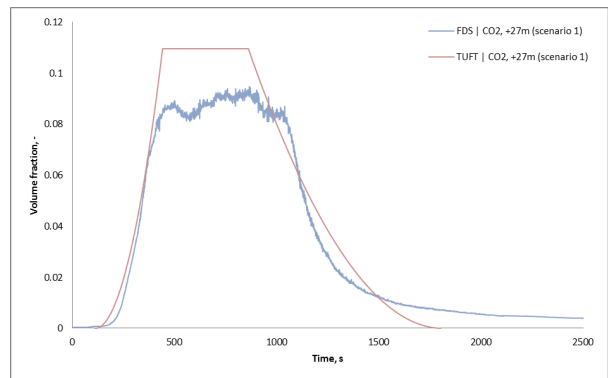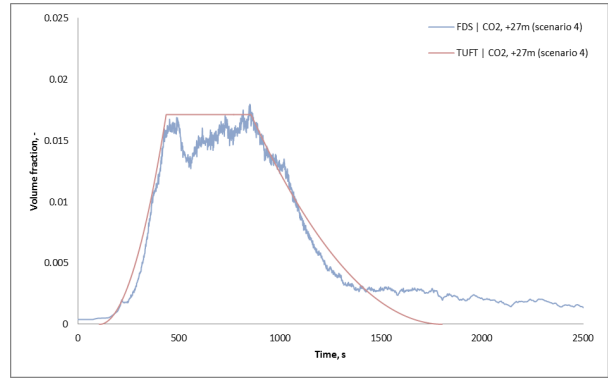

Figure 67. The volume fraction of carbon dioxide measured 27 m downstream the fire source.
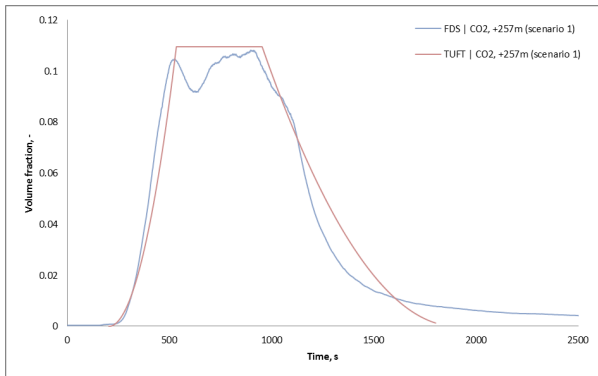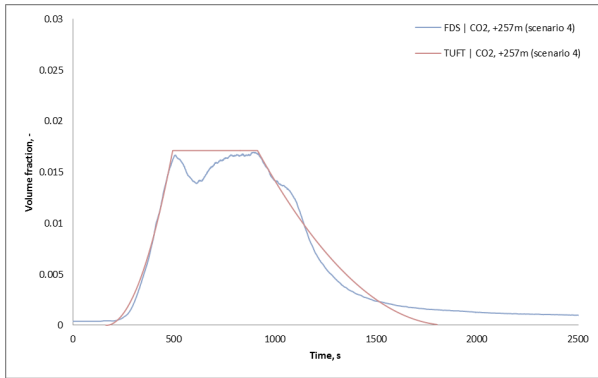

Figure 68. The volume fraction of carbon dioxide 257 m downstream the fire source.
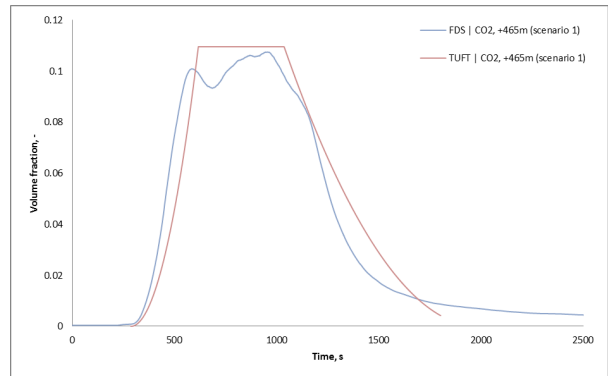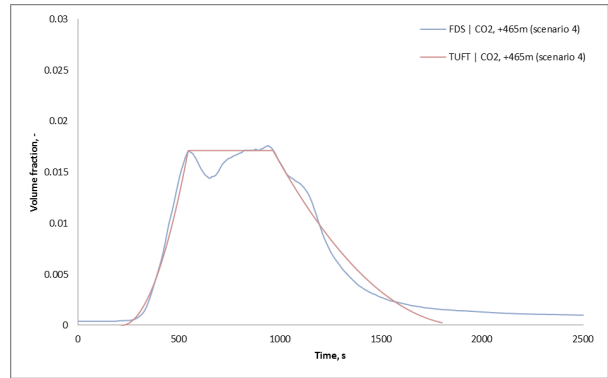

Figure 69. The volume fraction of carbon dioxide measured 465 m downstream the fire source.
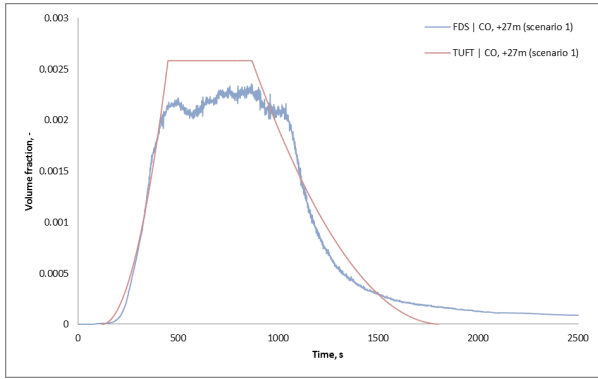
Figure 70. The volume fraction of carbon monoxide measured 27 m downstream the fire source.
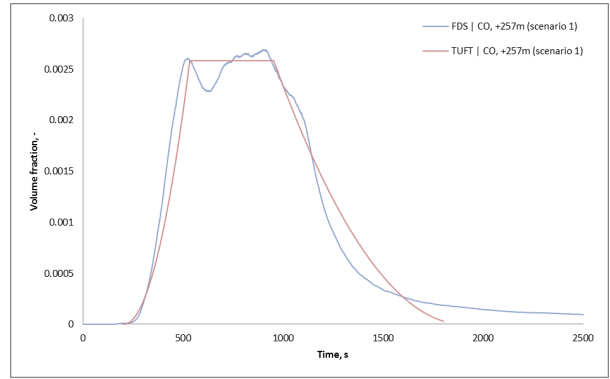
Figure 71. The volume fraction of carbon monoxide measured 257 m downstream the fire source.
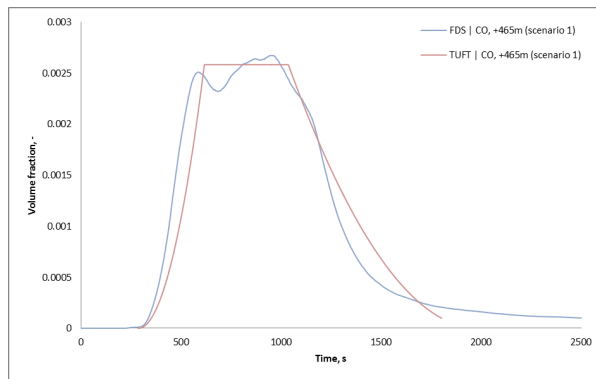
Figure 72. The volume fraction of carbon monoxide measured 465 m downstream the fire source.

Extinction Coefficient
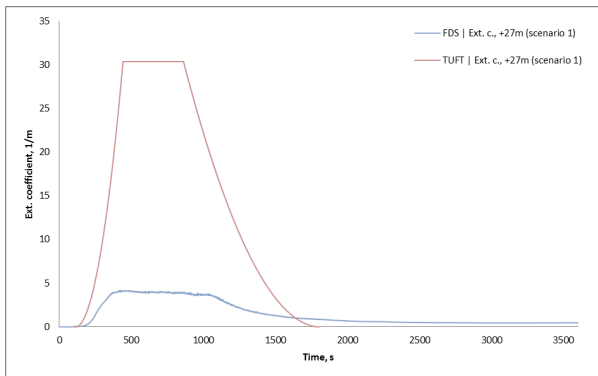
Figure 73. The extinction coefficient measured 27 m downstream the fire source.
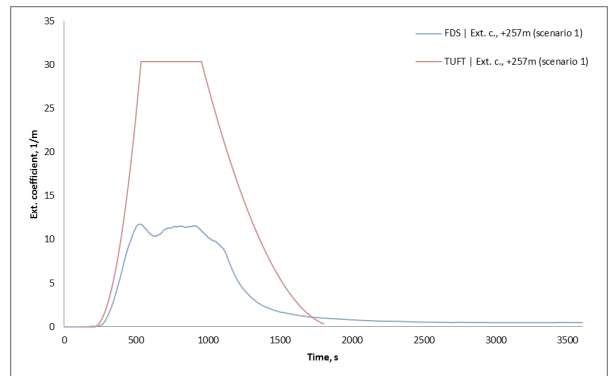
Figure 74. The extinction coefficient measured 257 m downstream the fire source.
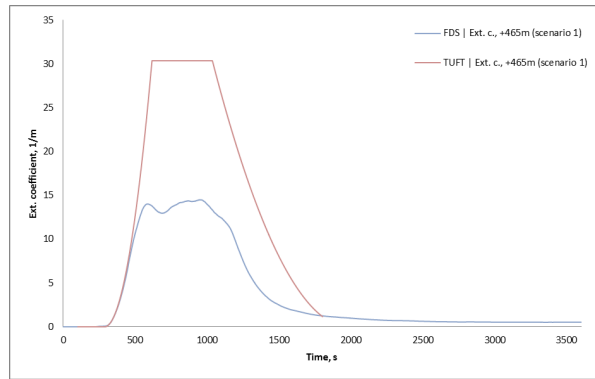
Figure 75 The extinction coefficient measured 465 m downstream the fire source.

Scenario 2 - Tunnel height 3 meters

Gas temperature
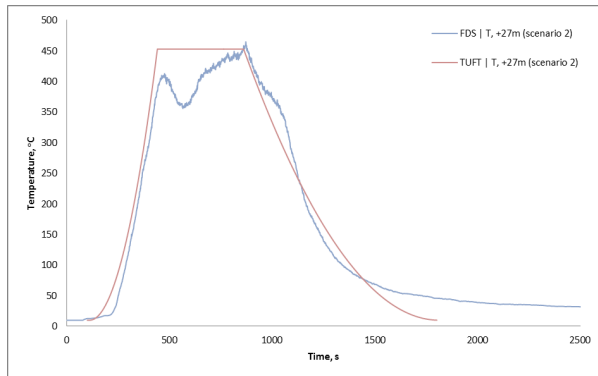
Figure 76. The gas temperature measured 27 m downstream the fire source.
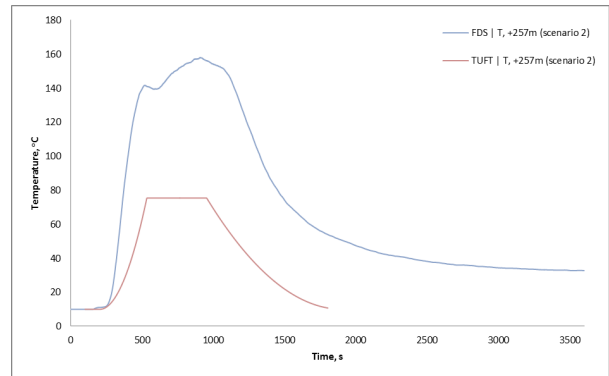
Figure 77. The gas temperature measured 257 m downstream the fire source.
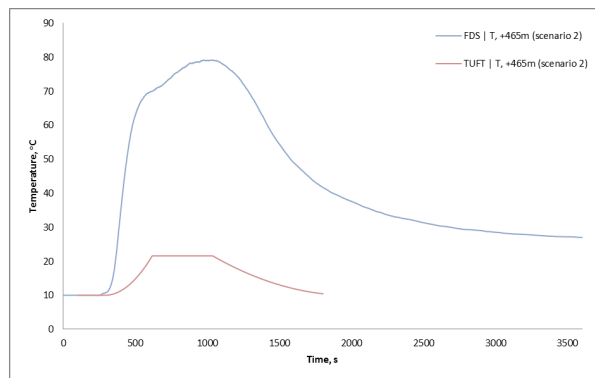
Figure 78 The gas temperature measured 465 m downstream the fire source.

Gas concentrations
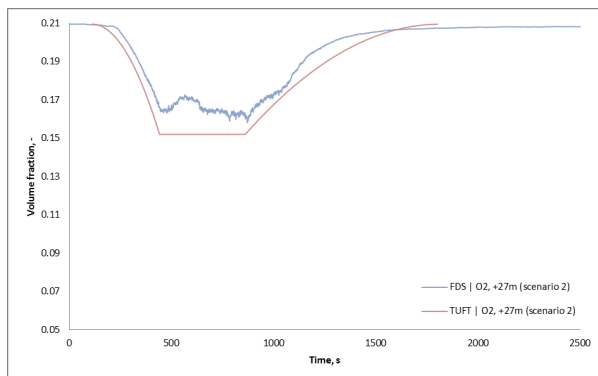
Figure 79. The volume fraction of oxygen measured 27 m downstream the fire source.
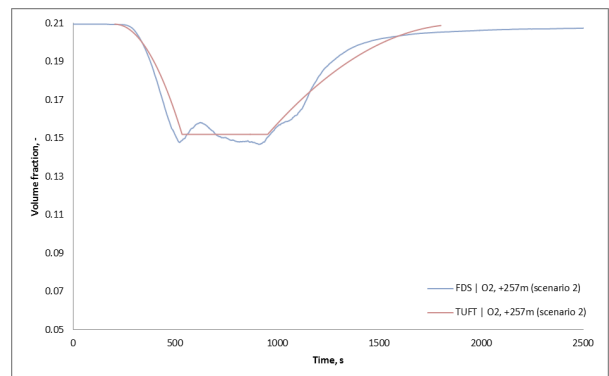
Figure 80. The volume fraction of oxygen 257 m downstream the fire source.
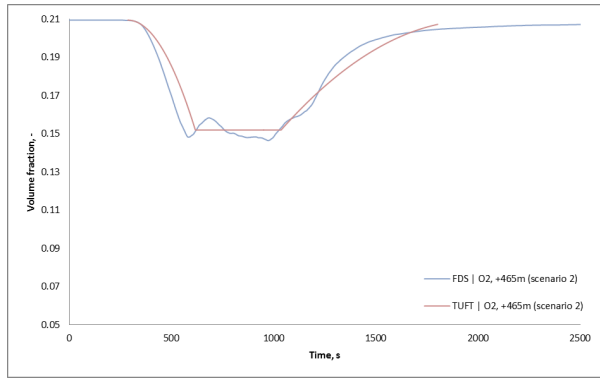
Figure 81. The volume fraction of oxygen 465 m downstream the fire source.
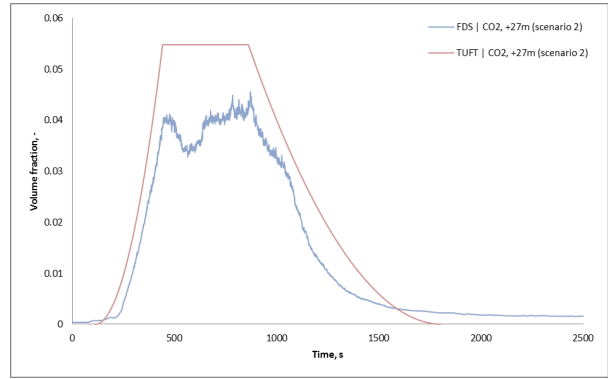
Figure 82. The volume fraction of carbon dioxide measured 27 m downstream the fire source.
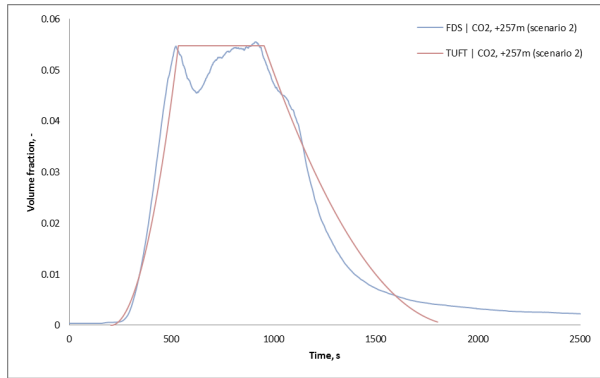
Figure 83. The volume fraction of carbon dioxide 257 m downstream the fire source.
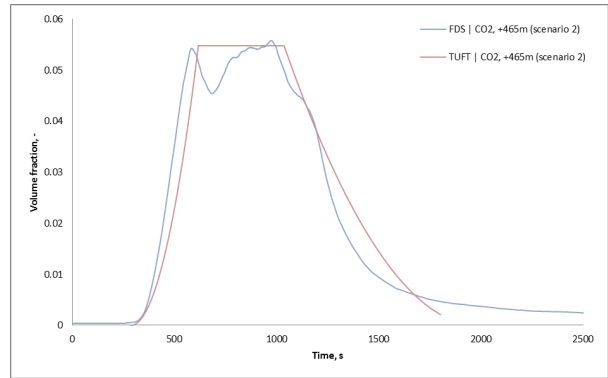
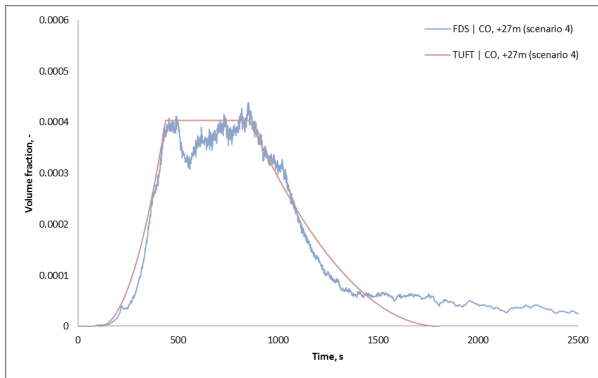Figure 84. The volume fraction of carbon dioxide measured 465 m downstream the fire source.
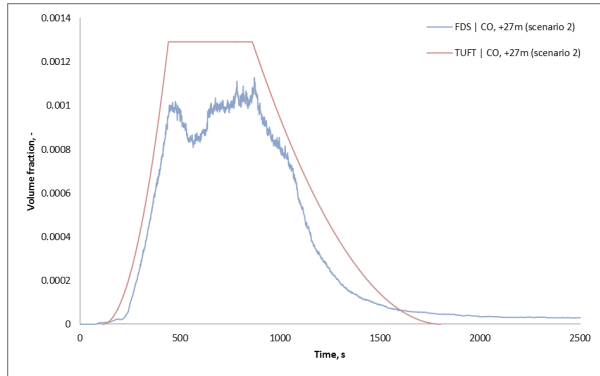
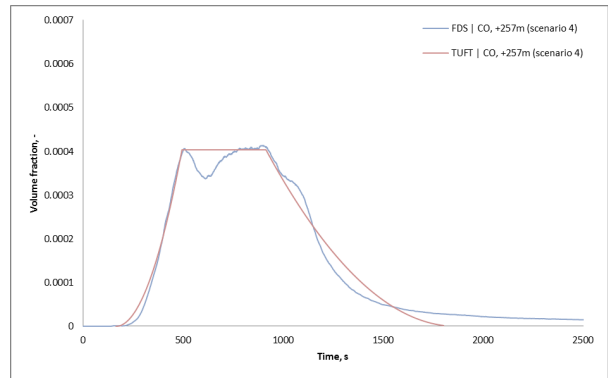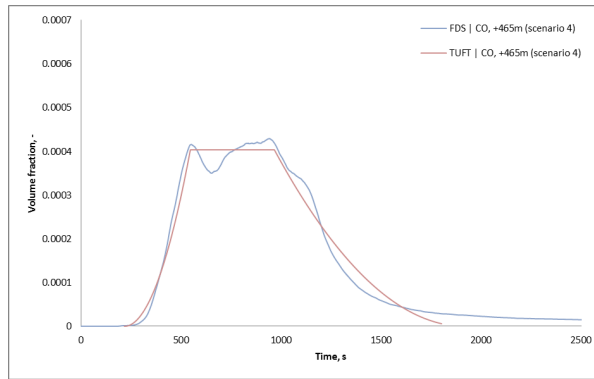Figure 85. The volume fraction of carbon monoxide measured 27 m downstream the fire source.
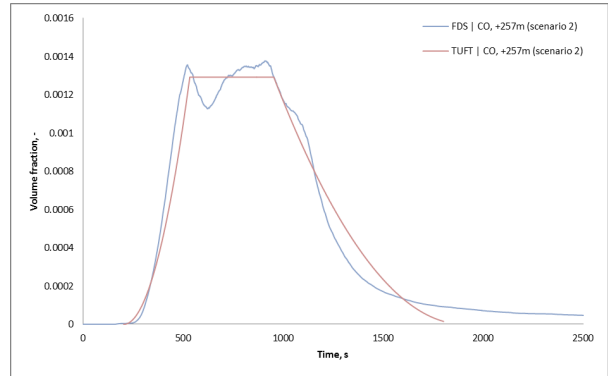
Figure 86. The volume fraction of carbon monoxide measured 257 m downstream the fire source.

VIII
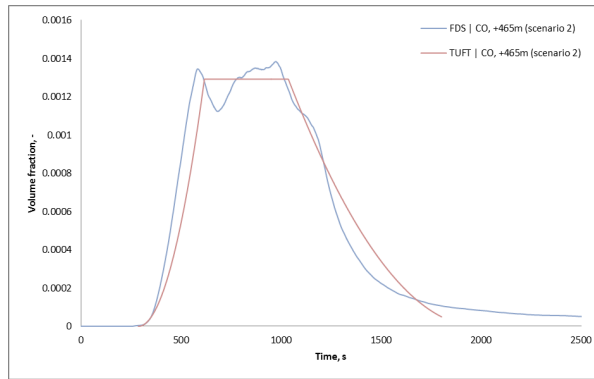
Figure 87. The volume fraction of carbon monoxide measured 465 m downstream the fire source.
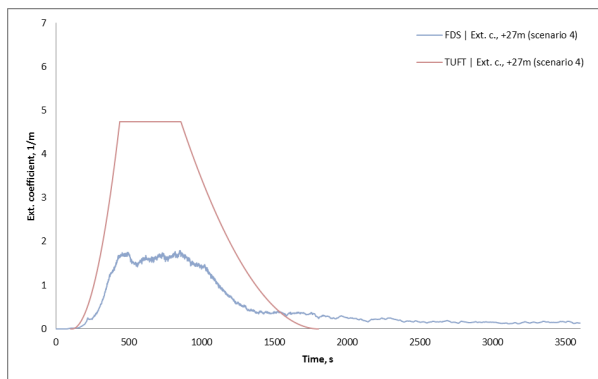
Extinction Coefficient
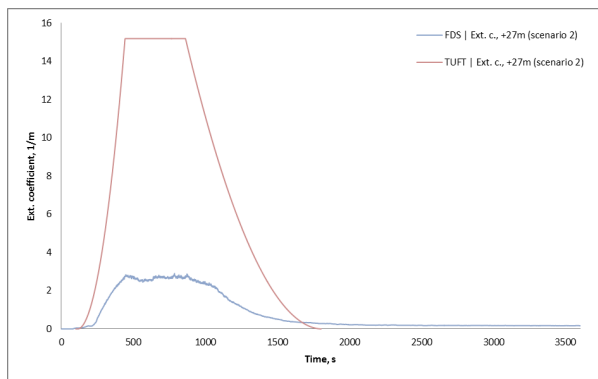
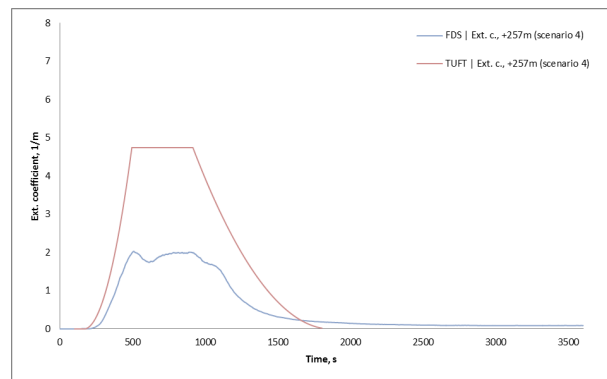Figure 88. The extinction coefficient measured 27 m downstream the fire source.
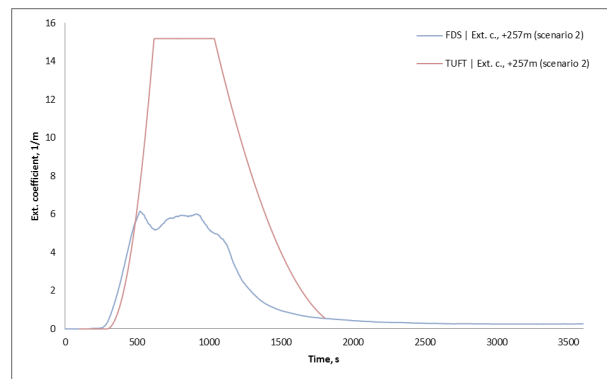
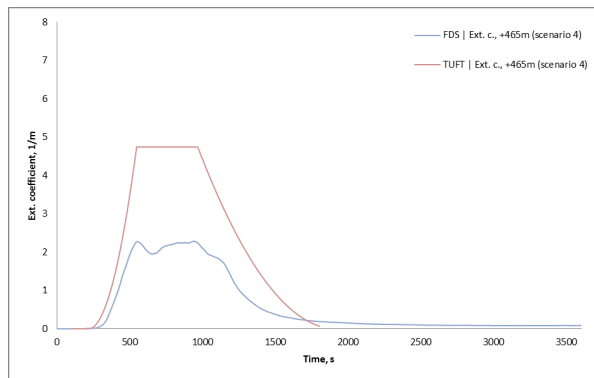Figure 89. The extinction coefficient measured 257 m downstream the fire source.
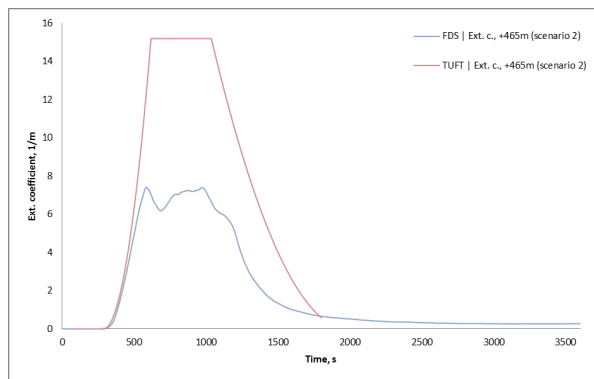
Figure 90 The extinction coefficient measured 465 m downstream the fire source.

X

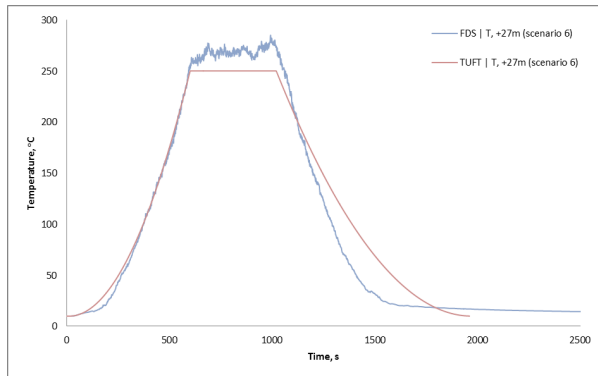# Scenario 4 – Wind speed 4 m/s

Gas temperature

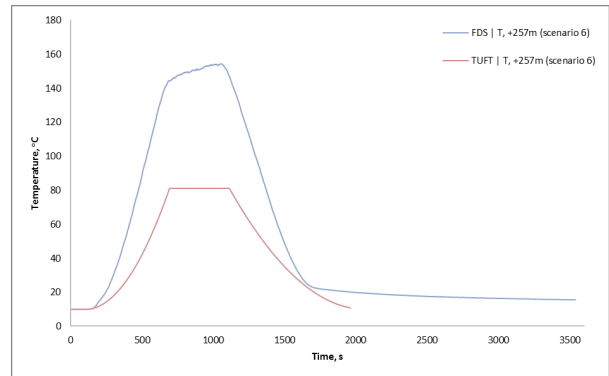Figure 91. The gas temperature measured 27 m downstream the fire source.

Figure 92. The gas temperature measured 257 m downstream the fire source.
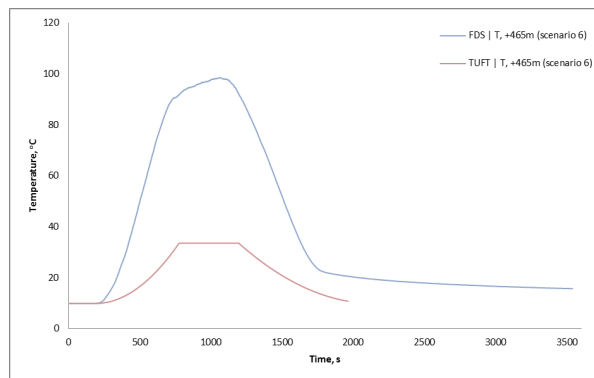

Figure 93 The gas temperature measured 465 m downstream the fire source.
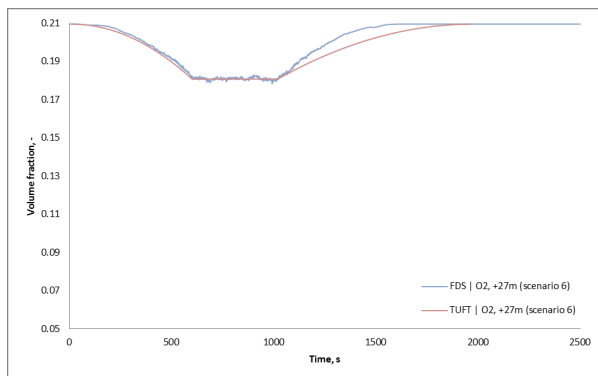
Gas concentrations

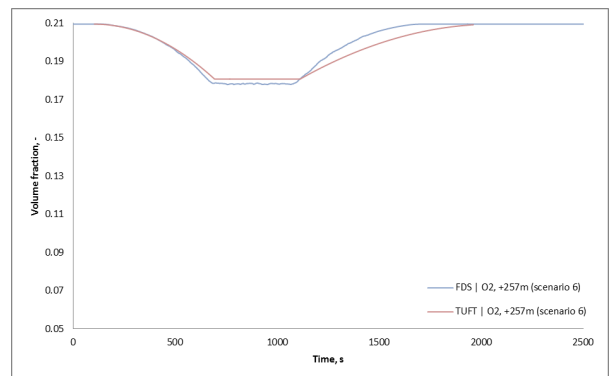Figure 94. The volume fraction of oxygen measured 27 m downstream the fire source.

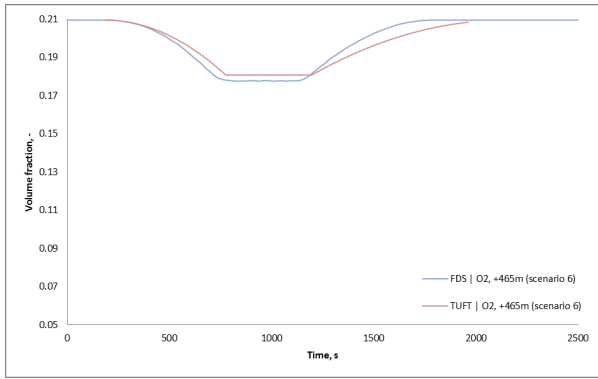Figure 95. The volume fraction of oxygen 257 m downstream the fire source.

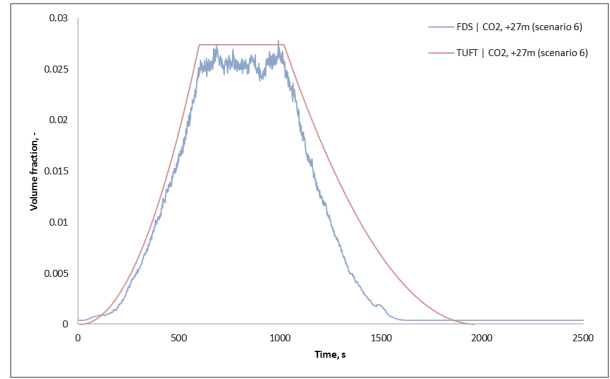Figure 96. The volume fraction of oxygen 465 m downstream the fire source.

Figure 97. The volume fraction of carbon dioxide measured 27 m downstream the fire source.
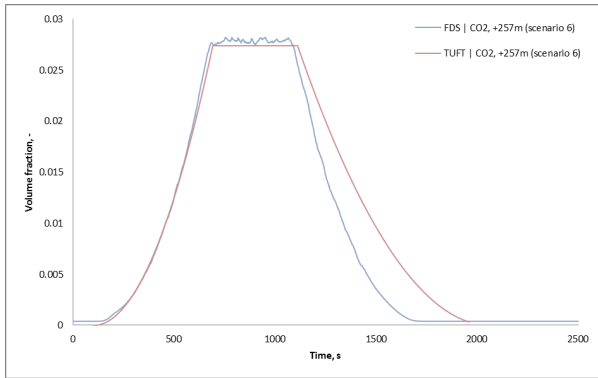

Figure 98. The volume fraction of carbon dioxide 257 m downstream the fire source.

Figure 99. The volume fraction of carbon dioxide measured 465 m downstream the fire source.

Figure 100. The volume fraction of carbon monoxide measured 27 m downstream the fire source.

Figure 101. The volume fraction of carbon monoxide measured 257 m downstream the fire source.

Figure 102. The volume fraction of carbon monoxide measured 465 m downstream the fire source.

Extinction Coefficient

Figure 103. The extinction coefficient measured 27 m downstream the fire source.

Figure 104. The extinction coefficient measured 257 m downstream the fire source.

Figure 105 The extinction coefficient measured 465 m downstream the fire source.

Scenario 6 – HRR growth rate 0.19 kW/s^2

Gas temperature

Figure 106. The gas temperature measured 27 m downstream the fire source.

Figure 107. The gas temperature measured 257 m downstream the fire source.

Figure 108 The gas temperature measured 465 m downstream the fire source.

Gas concentrations

Figure 109. The volume fraction of oxygen measured 27 m downstream the fire source.

Figure 110. The volume fraction of oxygen 257 m downstream the fire source.

Figure 111. The volume fraction of oxygen 465 m downstream the fire source.

Figure 112. The volume fraction of carbon dioxide measured 27 m downstream the fire source.

Figure 113. The volume fraction of carbon dioxide 257 m downstream the fire source.
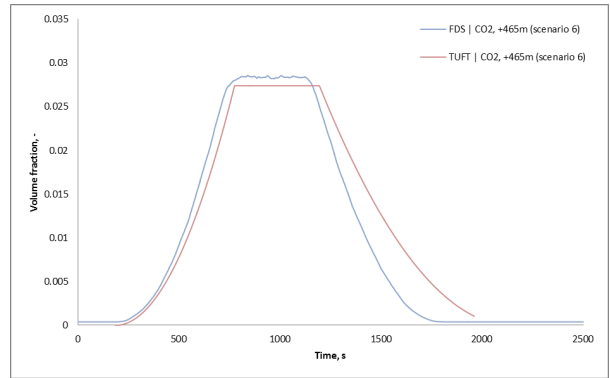

Figure 114. The volume fraction of carbon dioxide measured 465 m downstream the fire source.
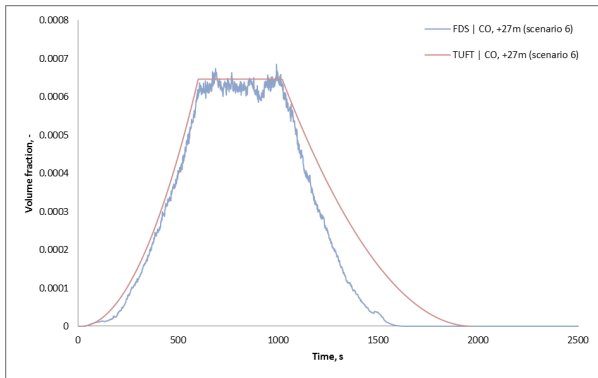

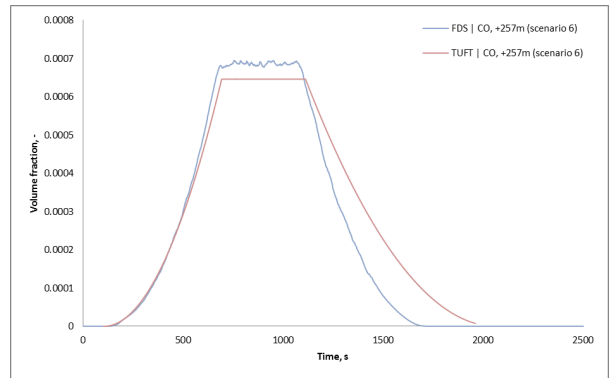Figure 115. The volume fraction of carbon monoxide measured 27 m downstream the fire source.

Figure 116. The volume fraction of carbon monoxide measured 257 m downstream the fire source.
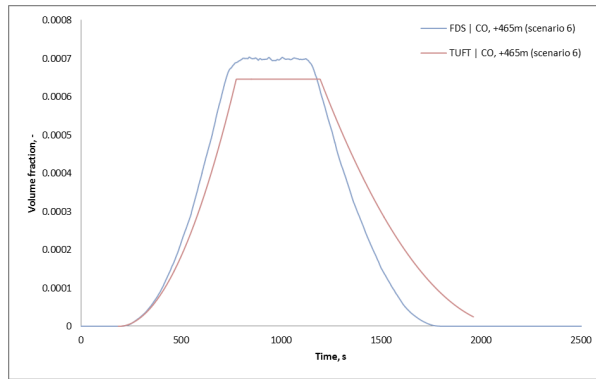
Figure 117. The volume fraction of carbon monoxide measured 465 m downstream the fire source.
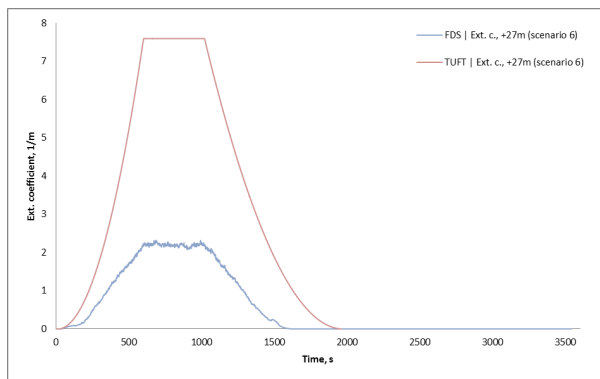
Extinction Coefficient

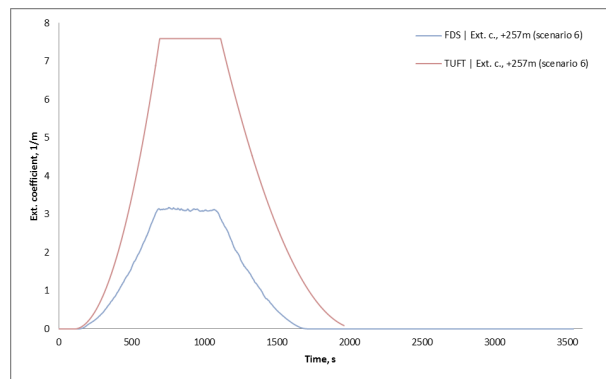Figure 118. The extinction coefficient measured 27 m downstream the fire source.

Figure 119. The extinction coefficient measured 257 m downstream the fire source.
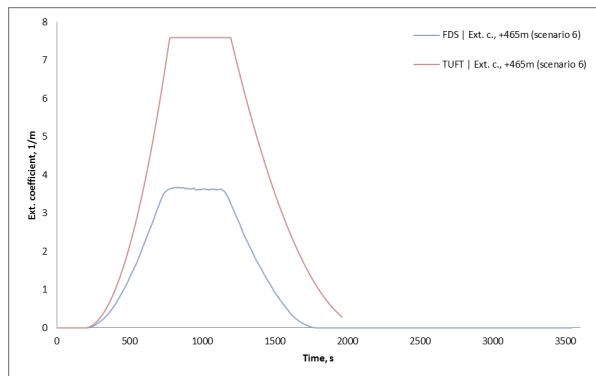

Figure 120 The extinction coefficient measured 465 m downstream the fire source.